Major Project

Dissertation on

"EXERGY ANALYSIS OF A DOUBLE EFFECT PARALLEL FLOW CHILLER"

Submitted to Delhi Technological University in partial fulfillment of the requirement for the award of Degree of

Master of Technology

In

Thermal Engineering

ABHISHEK SHARMA

2K13/THE/02

UNDER THE SUPERVISION OF

Mr.N.A. Ansari

Asst. Professor

Department Of Mechanical Engineering

Delhi Technological University

Delhi-110042

Department of Mechanical Engineering
Delhi Technological University
(Formerly Delhi College of engineering)
Bawana Road, Delhi-110042

2015

CERTIFICATE

DELHI TECHNOLOGICAL UNIVERSITY
(Formerly DELHI COLLEGE OF ENGINEERING)

Date:-_____

This is to certify that report entitled **"EXERGY ANALYSIS OF A DOUBLE EFFECT PARALLEL FLOW CHILLER"** by **ABHISHEK SHARMA** is the requirement of the partial fulfillment for the award of Degree of **Master of Technology (M.Tech)** in **Thermal Engineering** at **Delhi Technological University**. This work was completed under my supervision and guidance. He has completed his work with utmost sincerity and diligence. The work embodied in this project has not been submitted for the award of any other degree to the best of my knowledge.

SUPERVISIOR
Mr.N.A.Ansari
Asst. Professor
Department of Mechanical Engineering
DELHI TECHNOLOGICAL UNIVERSITY

ACKNOWLEDGEMENT

First of all, I would like to express my gratitude to God for giving me ideas and strengths to make my dreams true and accomplish this thesis.

To achieve success in any work, guidance plays an important role. It makes us put right amount of energy in the right direction and at right time to obtain the desired result. Express my sincere gratitude to my guide, **Mr. N.A. Ansari**, Asst.Professor, Mechanical Engineering Department for giving valuable guidance during the course of this work, for his ever encouraging and timely moral support. His enormous knowledge always helped me unconditionally to solve various problems.

I am greatly thankful to **Prof. R.S. Mishra**, Professor and Head, Mechanical Engineering Department, Delhi Technological University, for his encouragement and inspiration for execution of the this work. I express my feelings of thanks to the entire faculty and staff, Department of Mechanical Engineering, Delhi Technological University, and Delhi for their help, inspiration and moral support, which went a long way in the successful completion of my report work.

ABHISHEK SHARMA

(Roll No-2K13/THE/02)

ABSTRACT

A 500 TR double effect parallel flow absorption chiller with H_20-LiBr as refrigerant-absorbent is studied and the exergy destruction at each of its components is calculated. In the parallel-flow cycle, a whole weak solution is sent to high temp generator by passing through the low temperature generator. Such type of arrangement in the double effect system increases COP of the cycle as compared to single effect cycle. A simulation analysis of its exergy destruction at each component has been done with the help of EES.

The results of simulation are used to study the influence of the various operating parameters such as generator, evaporator and condenser temperatures on the exergy destruction in absorber, condenser, evaporator, high temperature regenerator, low temperature regenerator, high temperature heat exchanger, low temperature heat exchanger, lower solution expansion valve, upper solution expansion valve, lower refrigerant expansion valve, upper refrigerant expansion valve and the overall system. The results can be useful in the design, control and the performance enhancement of these absorption chillers.

Keywords*:* double effect, absorption etc.

CONTENTS

LIST OF FIGURES

LIST OF TABLES

NOMENCLATURE

EVP	Evaporator
CON	Condenser
ABS	Absorber
HTRG	High Temperature Regenerator
LTRG	Low Temperature Regenerator
USEV	Upper Solution Expansion Valve
LSEV	Lower Solution Expansion Valve
UREV	Upper Refrigerant Expansion Valve
LREV	Lower Refrigerant Expansion Valve
HTHE	High Temperature Heat Exchanger
LTHE	Low Temperature Heat Exchanger
H E	Heat Exchanger
HX	Heat Exchanger
CG	Condenser Generator
HPG	High Pressure Generator
LPG	Low Pressure Generator
RDR	Refrigeration Distribution Ratio
Ex Des	Exergy Destruction
COP	Coefficient Of Performance

SYMBOLS

Letters	Description	Unit
$\dot{m}$	Mass flow rate	kg/s
η_{ex}	Exergetic Efficiency	-
h	Enthalpy	kJ/kg
P	Pressure	kPa
T	Temperature	K
S	Entropy	kJ/kg-^{o}K
Q	Heat Energy	kW

CHAPTER 1

INTRODUCTION

1.1 INTRODUCTION TO ABSORTION SYSTEM

Recently, interest has been growing in absorption refrigeration technology because the conventional refrigeration and air conditioning systems have high grade energy consumption and also they contribute to the ozone layer depletion and green house effect. Absorption cooling systems are energy-efficient and environmentally friendly compared to CFC-based vapor compression systems. These systems use low grade energy such as waste energy in fuel cells, residual heat from engines, large power plants and factories. Low grade energy is also available from other sources such as solar, biomass, geothermal etc. These machines also eliminate the concerns about lubricants which is mixed with refrigerants. Absorption system has less efficiency compared to vapor compression system but by increasing the number of effects in absorption systems, the performance can be improved. Single effect cycles cannot make effective use of higher temperature heat sources. An increment in the number of effects leads to a higher efficiency in the system because it increases the number of times, the heating power provided by the heat source that is used in the system. When the number of effects is increased, COP of each effect will not be as high as that for a single effect system. Also, higher number of effects will lead to more complexity in the system.

Double effect absorption cycles are classified as series flow, parallel flow and reverse parallel flow, depending on the solution flow. A large no of industrial process uses lot of thermal energy by burning fossil fuel to produce steam or heat for their operation. After the processes, heat is rejected as waste to the surrounding. This waste heat can be utilized for refrigeration by using a heat operated refrigeration system, such as an absorption refrigeration cycle. Despite a lower coefficient of performance (COP) as compared to the vapor compression system, absorption refrigeration systems are promising for using waste energy from industrial processes, geothermal energy, solar energy etc.

1.2 SIMPLE VAPOUR ABSORPTION SYSTEM

A single-effect absorption cooling system consists of an absorber (A), a generator (G), a condenser (C), an evaporator (E), two valves, a heat exchanger (HE) and a pump as can be seen in Fig. 1. The cycle has two circuits: the refrigerant circuit and solution circuit. Heat is

supplied to the generator to separate part of the refrigerant from the solution at high pressure and temperature; once the refrigerant is evaporated, it is passed to the condenser where it is liquefied releasing heat to the atmosphere. The refrigerant in liquid phase is then passed through the expansion valve reducing its pressure and temperature. Then, the liquid vapor mixture is led to the evaporator where the refrigerant absorbs heat producing the cooling effect. The refrigerant vapor leaving the evaporator goes to the absorber where it is absorbed by the absorbent solution coming from the generator. This solution is pumped to the generator starting the cycle again. A solution heat exchanger is placed between the absorber and the generator to recover heat from the solution going from the generator to the absorber.

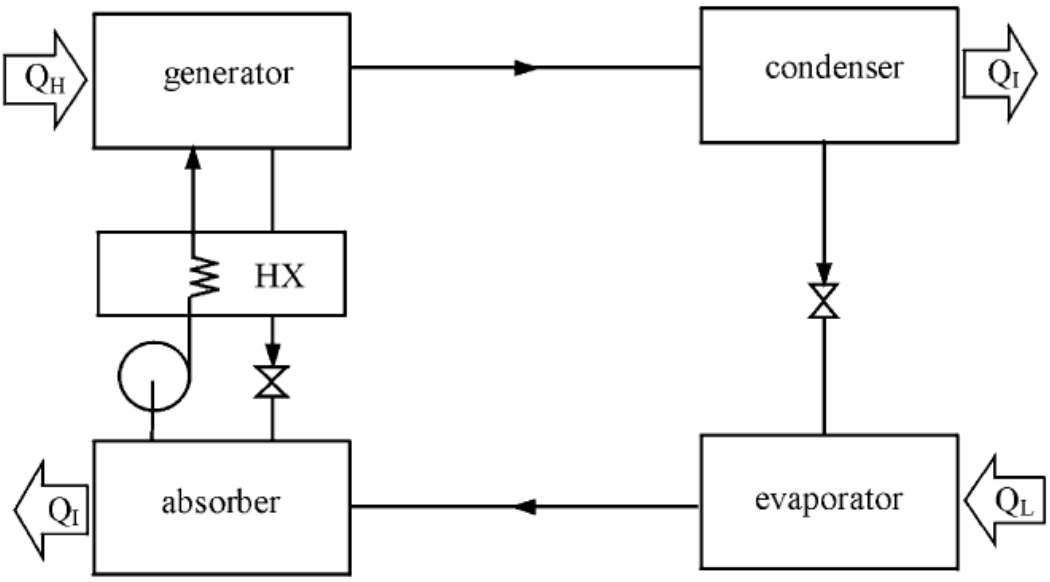

Fig:1.1 A single-effect absorption refrigeration system with a solution heat exchanger[1]

1.3 DOUBLE EFFECT VAPOUR ABSORPTION SYSTEM IN SERIES

A double-effect in series system, compared with the single effect, consists of the following extra components at high pressure: a generator, a condenser, and a heat exchanger. The objective of adding the components mentioned above is to improve the COP of the system. In this system, the refrigerant vapor is produced in both the generator (G) and the condenser-generator (CG) at high and intermediate pressures, respectively, and the solution with high refrigerant concentration goes directly from the absorber to the generator passing through the

heat exchangers. In this system, heat is only supplied to the generator at high temperature in order to produce the refrigerant vapor. The refrigerant vapor, produced in the generator goes to the condenser-generator (CG) to be liquefied. In this component, the heat delivered during the condensation is used to produce more refrigerant vapor at intermediate pressure which is then condensed in the condenser. The two streams with the liquid refrigerant join at intermediate pressure and pass through the expansion valve to the evaporator to produce the cooling effect. The refrigerant leaving the evaporator goes to the absorber where it is absorbed by the solution coming from the condenser-generator. Finally, the high concentration solution is pumped to the generator through the heat exchangers starting the cycle again.

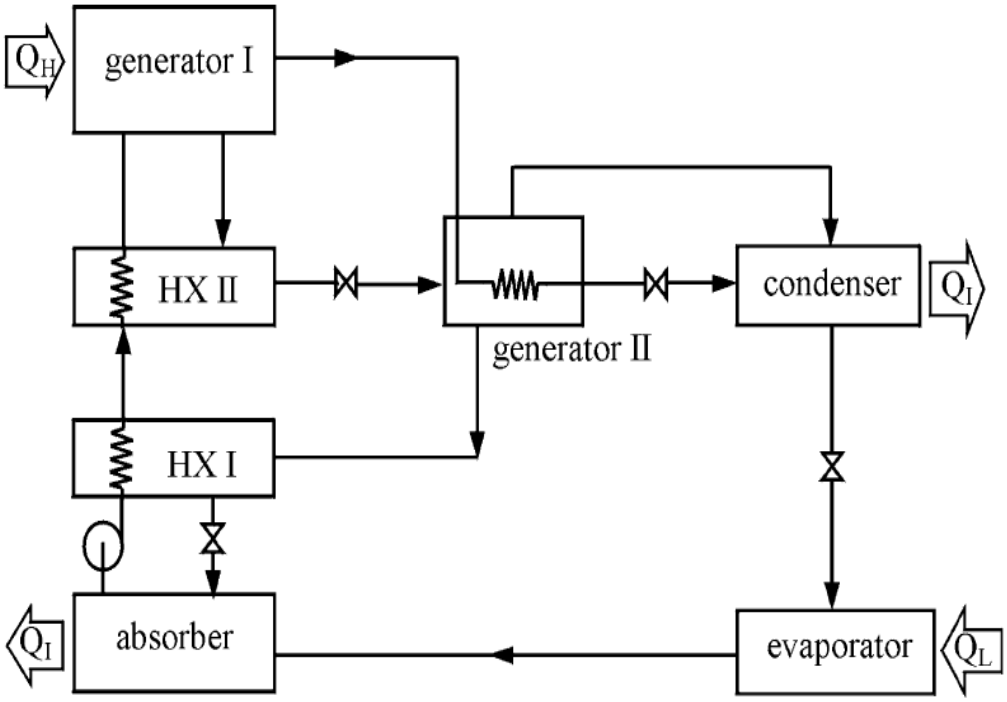

Fig.1.2. Double-effect in series absorption cooling system[1]

1.4 DOUBLE EFFECT VAPOUR ABSORPTION SYSTEM IN PARALLEL

In this system, two separate loops are there in the low temperature regenerator. One loop is heated to state point 5 and superheated steam is generated at state point 8 and the other loop indirectly is heated to state point 11. After an expansion valve, state point 6 reduces its pressure to the two-phase mixture region at state point 7. High temperature superheated steam is provided at state point 17 which then enters the low temperature regenerator to provide

superheated steam at state point 8. Superheated steam at state point 17 is condensed to saturated liquid water at state point 18. A refrigerant expansion valve is used to reduce the pressure at state point 18 to the intermediate pressure, so state point 19 is in the two phase region. The vapor part of the flow at state point 19 combines with the superheated flow at state point 8, and is then condensed (in the condenser) to form saturated liquid water at state point 9.

The liquid part of the flow at state point 10 is heated by the building loop to saturated water vapor. This water vapor is combined with the vapor part of state point 10 to form state point1. The water vapor at state point 1 is absorbed by the strong solution from state point 7 to become the dilute solution in state point 2, thus completing the cycle.

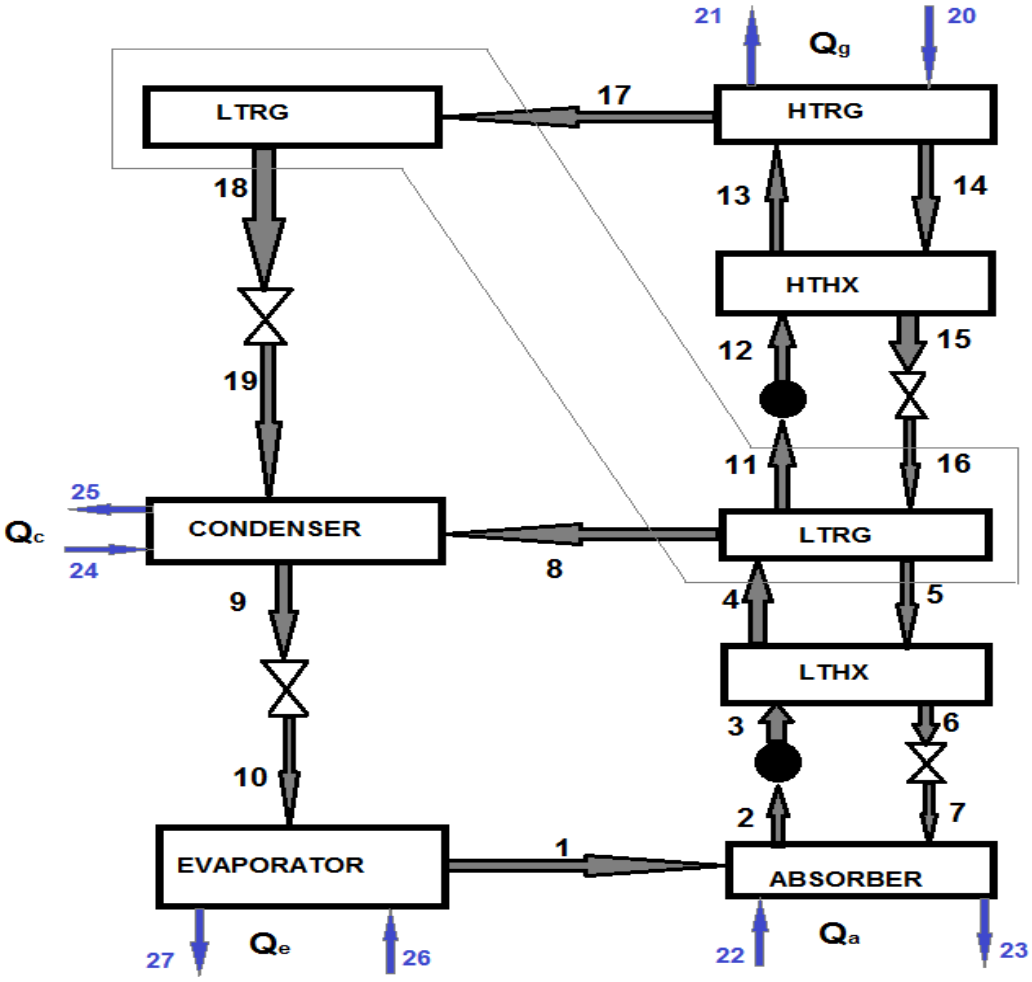

Fig.1.3 Double-effect in parallel absorption cooling system.

CHAPTER 2
LITERATURE REVIEW

In recent years, a number of researchers have investigated double effect vapor absorption systems using energy analysis approach. In 1996, Xu and Dai carried out a thermodynamic analysis to study the series flow double effect absorption chiller using LiBr/water as working fluid and in 1997 they studied parallel flow double effect cycle in the same manner. In 2000, Arun etal studied the double effect series flow absorption refrigeration system with emphasis on estimation of LPG temperatures and in 2001 they compared parallel flow and series flow cycles based on first law analysis. In 2004 Liu and Wang designed a new kind of solar/gas driving double effect parallel flow LiBr/water absorption system. They studied this cycle from the view point of first law of thermodynamics and in order to acquire a more detailed comparison of some alternative systems, several refrigeration and heat pump systems were compared with each other.The economic evaluation illustrated that their new system yields good economic returns. In 2006 Manohar etal,used neural network for modelling a double effect, series flow absorption chiller.

In 2009, Torrella etal presented a procedure for calculating the COP and heat transfer rates based on on-site experimental temperature measurements of a LiBr/water double effect chiller in reverse parallel configuration. In 2009 Maria Puig-Arnavat et al compared two approaches to the characteristics equation method in order to find a simple model that best describes the performance of thermal chillers. After obtaining the results for single effect chiller, they choose the characteristic equation method developed by Kuhn and Ziegler and extended it to double effect commercial chillers.

In 2008 Gomri and Hakimi studied the series flow double effect absorption cooler. Their study was very limited and only the effect of HPG and LPG temperatures on COP and second law efficiency was investigated. Again in 2009 Gomri extended his study on series flow double effect absorption cycle. Also he analyzed single effect cycle and compared them with each other in several conditions.

In 2009 Kaushik and Arora did a similar work to Gomri's study, however, their study was more extended. But, it was limited to series flow system and also, the effect of some important parameters like evaporator temperature or pressure drop between LPG and

condenser and etc were not considered. L. Garousi Farshi, S. M. Seyed Mahmoudi have done the performance comparison of double effect cycle with series.parallel and reverse flow taking H_2O-LiBr.

Saeed Sedigh and Hamid Saffari have performed thermodynamic analysis of Series and Parallel Flow Water/Lithium bromide double effect absorption system with two condensers. The results show that the coefficient of performance of the parallel-flow double-effect cycle is higher than the coefficient of performance of series-flow double-effect cycle. Also the heats exchanged in series cycle are higher than that in parallel cycle.

L.A. Domínguez-Inzunza, J.A. Hernández-Magallanes, M. Sandoval-Reyes,& W. Rivera Compare the performance of single-effect, half-effect, double effectin series and inverse and triple-effect absorption cooling systems operating with the NH_3-$LiNO_3$ mixture.they found that with double-effect systems it is possible to obtain coefficients of performance as high as 1.12 but they need generator temperatures higher than 140 °C to get good values of the coefficients of performance. Finally, the highest coefficients of performance can be achieved with triple-effect systems but they require the highest generator temperatures (starting from 150°C), they are the most complex and they should be mainly used for air conditioning.

Mohammad Seraj & M. Altamush Siddiqui have done the performance analysis of parallel flow Single and double effect absorption cycles. Their result show that In the single effect cycle using HRA, with refrigerant parallel flow, COP increases with increase in the values of refrigeration distribution ratio (RDR). The optimum value obtained is, RDR =0.3. In the double effect parallel and series flow cycles, COP increases more drastically with increase in the high pressure generator temperature (Tg) as compared to the single effect cycle.

J. Rasson,K.EaoM,Wahlig have performed analysis on The Double-Effect Regenerative Absorption Heat Pump. R. Palacios Bereche, R. Gonzales Palomino, S. A. Nebra have done thermoeconomic analysis of a single and double-Effect LiBr/H_2O absorption refrigeration system. They found that from the standpoint of the exergetic analysis,single-effect absorption refrigeration systems are suitable to operate in cogeneration systems or using as fuel some waste heat at low temperature (higher than 80°C but lower than 120°C).On the other hand, double effect systems have a better exergetic performance for either direct-fired or steamdriven, but they need higher temperatures to operate.

G. Subba Rao, Vemuri Lakshminarayana have performed the Simulation and Analysis of Biogas operated Double Effect GAX Absorption Refrigeration System.their result show that Moderate HT generator pressures and lower temperatures yield good results and better performance of the system. Similarly lower HT generator temperatures result in reduced requirements of energy inputs and hence low quantities of biogas is sufficient to power the absorption cycle.

Christopher Somers has done simulation of absorption cycles for integration into refining processes. an analysis was done to evaluate which chiller design was the most utile. This analysis concluded that for this application, a double effect water/LiBr chiller is the best design to use.

Luis González, Nicolás Velázquez, Adolfo Ruelas, Gabriel Pando, Mydory Nakasima have done modelling and simulation of a double effect absorption system LiBr-H2O of low capacity activated with solar energy. According to the simulation performed best operation conditions for a load of 16 kW in the evaporator, activation requires a temperature in the high temperature generator approximately 150 ° C which are easily reached by the heat generated from the burning of biogas (800-1000 ° C) and the placement of solar thermal collectors as low and medium temperature are evacuated tube collectors (50-200 ° C), compound parabolic collector (67-287 ° C), Fresnel reflector (67 - 267 ° C) and parabolic cylinder (67-267 ° C).

CHAPTER 3

EXERGY ANALYSIS OF DOUBLE EFFECT PARALLEL FLOW SYSTEM

3.1 ASSUMPTIONS

i. Thermodynamic equilibrium is there throughout the entire system.

ii. The analysis is made under steady state conditions.

iii. A rectifier is unnecessary since the absorbent does not evaporate in the temperature range under consideration.

iv. Solution is at saturated state when leaving generator and absorber, and refrigerant is at saturated state when leaving condenser and evaporator.

v. Heat losses and pressure drops in the tubing and the components are considered negligible.

vi. Pump work is neglected.

3.2 SYSTEM DESCRIPTION

The system consists of following components:-

1. Absorber

2. Condenser

3. Evaporator

4. High Temperature Regenerator

5. Low Temperature Regenerator

6. High Temperature Heat Exchanger

7. Low Temperature Heat Exchanger

8. Lower Solution Expansion Valve

9. Upper Solution Expansion Valve

10.Lower Refrigerant Expansion Valve

11.Upper Refrigerant Expansion Valve

12.Lower Solution Pump

13.Upper Solution Pump

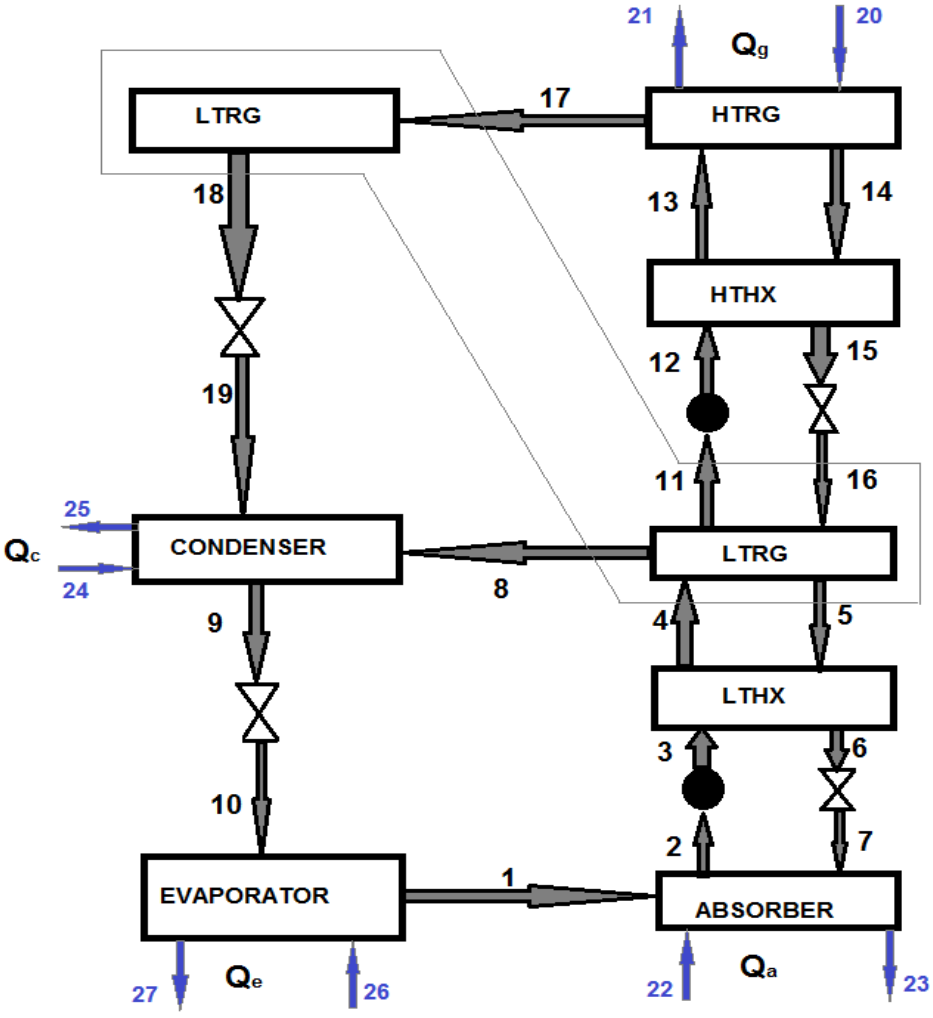

Fig.3.1 Double Effect Parallel Flow System

The low concentration solution at state point 2 is pumped to increase its pressure to state point 3 where it enters the low temperature heat exchanger and is heated to state point 4 which then enters the low temperature regenerator. Two separate loops are there in the low temperature regenerator. One loop is heated to state point 5 and superheated steam is generated at state point 8 and the other loop indirectly is heated to state point 11.The solution at state point 11 is pumped to high temperature regenerator by passing through the high temperature heat exchanger. In the high temperature regenerator, heat is supplied from an external heat source such as waste steam to produce the refrigerant vapor at state point 17 and high concentration solution at state point 14 respectively. The solution at state 14 is then passed to the high temperature heat exchanger and then to the upper solution expansion valve. It then enters the low temperature regenerator at state point 16. After an expansion valve, state point 6 reduces its pressure to state point 7. High temperature superheated steam is provided at state point 17 which then enters the low temperature regenerator to provide superheated steam at state point 8. Superheated steam at state point 17 is condensed to saturated liquid water at state point 18. A refrigerant expansion valve is used to reduce the pressure at state point 18 to the intermediate pressure, so state point 19 is in the two phase region. The vapor part of the flow at state point 19 combines with the superheated flow at state point 8, and is then condensed (in the condenser) to form saturated liquid water at state point 9 which then passed through an expansion valve to reach state point 10.The liquid part of the flow at state point 10 is heated by the building loop to saturated water vapor. This water vapor is combined with the vapor part of state point 10 to form state point1. The water vapor at state point 1 is absorbed by the strong solution from state point 7 to become the dilute solution in state point 2, thus completing the cycle.

3.3 GOVERNING EQUATIONS

m, T, h, S and x stands for mass flow rate, temperature, enthalpy, entropy and LiBr mass concentration respectively at different state points. T_o is the atmospheric temperature.

1. Evaporator

mass balance equation:

$m_{27} = m_{26}$

$m_{10} = m_1$

energy balance equation:

$Q_{EVP} = m_{10}*(h_1 - h_{10})$

$Q_{EVP} = m_{26}*(h_{26} - h_{27})$

2. Condenser

mass balance equation:

$m_{24} = m_{25}$

$m_9 = m_8 + m_{19}$

energy balance equation:

$Q_{CON} = m_8*h_8 + m_{19}*h_{19} - m_9*h_9$

$Q_{CON} = m_{24}*(h_{25}-h_{24})$

3. Absorber

mass balance equation:

$m_{22} = m_{23}$

$m_2 = m_1 + m_7$

solute mass balance equation:

$m_2*x_2 = m_7*x_7$

energy balance equation:

$Q_{ABS} = m_1*h_1 + h_7*m_7 - m_2*h_2$

$Q_{ABS} = m_{22}*(h_{23} - h_{22})$

4. High Temperature Regenerator

mass balance equation:

$m_{20} = m_{21}$

$m_{13} = m_{14} + m_{17}$

solute mass balance equation:

$m_{13}*x_{13} = m_{14}*x_{14}$

energy balance equation:

$Q_{HTRG} = m_{17}*h_{17} + m_{14}*h_{14} - m_{13}*h_{13}$

$Q_{HTRG} = m_{20}*(h_{20} - h_{21})$

5. Low Temperature Regenerator

mass balance equation:

$m_{17} = m_{18}$

$m_4 + m_{16} = m_5 + m_{11} + m_8$

solute mass balance equation:

$m_4*x_4 + m_{16}*x_{16} = m_5*x_5 + m_{11}*x_{11}$

energy balance equation:

$h_4*m_4 + m_{16}*h_{16} + m_{17}*h_{17} = h_5*m_5 + h_{11}*m_{11} + m_{18}*h_{18} + m_8*h_8$

6. Lower Refrigerant Expansion Valve

mass balance equation:

$m_{10} = m_9$

solute mass balance equation:
$m_{10}*x_{10} = m_9*x_9$

energy balance equation:
$h_{10} = h_9$

7. Upper Refrigerant Expansion Valve
mass balance equation:
$m_{18} = m_{19}$
solute mass balance equation:
$m_{18}*x_{18} = m_{19}*x_{19}$

energy balance equation:
$h_{18} = h_{19}$

8. Lower Solution Expansion Valve
mass balance equation:
$m_6 = m_7$
solute mass balance equation:
$m_6*x_6 = m_7*x_7$

energy balance equation:
$h_6 = h_7$

9. Upper Solution Expansion Valve
mass balance equation:
$m_{15} = m_{16}$
solute mass balance equation for the upper solution expansion valve is:
$m_{15}*x_{15} = m_{16}*x_{16}$

energy balance equation for the upper solution expansion valve is:
$h_{15} = h_{16}$

10. High Temperature Heat Exchanger
mass balance equation:
$m_{12} = m_{13}$
$m_{14} = m_{15}$
solute mass balance equation:
$m_{12}*x_{12}=m_{13}*x_{13}$
$m_{14}*x_{14} = m_{15}*x_{15}$

energy balance equation:
m11*(h13 - h12) = m14*(h14 - h15)

11. Low Temperature Heat Exchanger

mass balance equation:

$m_3 = m_4$

$m_5 = m_6$

solute mass balance equation:

$m_3 * x_3 = m_4 * x_4$

$m_5 * x_5 = m_6 * x_6$

energy balance equation:

$m_2 * (h_4 - h_3) = m_5 * (h_5 - h_6)$

12. COP of The System

COP of the system is the ratio of the cooling effect from the evaporator to the thermal energy supplied in the high temperature regenerator.

COP=Qevap/Qgenh

COPe=Qevap/(Qgenh+0.5)

3.4 EXERGY DESTRUCTION EQUATIONS

1. The exergy destruction in the evaporator:

$ExDes_{EVP} = m_{26} * [(h_{26} - h_{27}) - T_o * (S_{26} - S_{27})] + m_{10} * [(h_{10} - h_1) - T_o * (S_{10} - S_1)]$

The exergy for the recquired cooling:

$Ex_{LOAD} = m_{26} * [(h_{26} - h_{27}) - T_o * (S_{26} - S_{27})]$

2.The exergy destruction in the condenser :

$ExDes_{CON} = m_{24} * [(h_{24} - h_{25}) - T_o * (S_{24} - S_{25})] + m_8 * (h_8 - T_o * S_8) + m_{19} * (h_{19} - T_o * S_{19}) - m_9 * (h_9 - T_o * S_9)$

The exergy loss from the condenser:

$ExLoss_{CON} = m_{24} * [(h_{25} - h_{24}) - T_o * (S_{25} - S_{24})]$

3. The exergy destruction in the absorber :

$ExDes_{ABS} = m_{22} * [(h_{22} - h_{23}) - T_o * (S_{22} - S_{23})] + m_1 * (h_1 - T_o * S_1) + m_7 * (h_7 - T_o * S_7) - m_2 * (h_2 - T_o * S_2)$

The exergy loss from the absorber:

$ExLoss_{ABS} = m_{22} * [(h_{23} - h_{22}) - T_o * (S_{23} - S_{22})]$

4. The exergy destruction in the high temperature regenerator:

$ExDes_{HTRG} = m_{20} * [(h_{20} - h_{21}) - T_o * (S_{20} - S_{21})] + m_{13} * (h_{13} - T_o * S_{13}) - m_{14} * (h_{14} - T_o * S_{14}) - m_{17} * (h_{17} - T_o * S_{17})$

The exergy supply:

$ExSupply_{HTRG} = m_{20} * [(h_{20} - h_{21}) - T_o * (S_{20} - S_{21})]$

5. The exergy destruction in the low temperature regenerator:

$ExDes_{LTRG} = m_{17}*[(h_{17} - h_{18})-T_o*(S_{17} - S_{18}))+m_4*(h_4 -T_o*S_4)+ m_{16}*(h_{16} -T_o*S_{16}) -m_{11}*(h_{11} - T_o*S_{11})- m_5*(h_5 -T_o*S_5) -m_8*(h_8 -T_o*S_8)$

6. The exergy destruction in the lower refrigerant expansion valve:

$ExDes_{VALVE,L,R} = m_9*T_o*(S_{10}- S_9)$

7. The exergy destruction in the upper refrigerant expansion valve :

$ExDes_{VALVE,H,R}= m_{18}*T_o*(S_{19} – S_{18})$

8. The exergy destruction in the lower solution expansion valve:

$ExDes_{VALVE,L,S}= m_6*T_o*(S_7 – S_6)$

9. The exergy destruction in the upper solution expansion valve:

$ExDes_{VALVE,H,S} = m_{15}*T_o*(S_{16} – S_{15})$

10. The exergy destruction in the high temperature heat exchanger:

$ExDes_{HTHX}=m_{12}*[(h_{12} - h_{13}) -T_o*(S_{12} - S_{13})] + m_{14}*[(h_{14} - h_{15})-T_o*(S_{14} - S_{15})]$

11. The exergy destruction in the low temperature heat exchanger:

$ExDes_{LTHX} = m_3*[(h_3 – h_4) -T_o*(S_3 – S_4)] + m_5*[(h_5 – h_6) -T_o*(S_5 – S_6)]$

The total exergy supplied to the system (to HTRG) is equal to the summation of the useful exergy to the load, the exergy destruction in each component and the exergy losses to the environment (through absorber and condenser):

$ExSupply_{HTRG}$ =

$Ex_{LOAD} + [ExDes_{EVP} + ExDes_{CON} + ExDes_{ABS} + ExDes_{HTRG} + ExDes_{LTRG} + ExDes_{VALVE,L,R}+ExDes_{VALVE,H,R}+ ExDes_{VALVE,L,S}+ExDes_{VALVE,H,S}+ ExDes_{LTHX} +ExDes_{HTHX}] +[ExLoss_{ABS}+ExLoss_{CON}]$

The system exergetic efficiency:

$\eta_{ex} = Ex_{LOAD}/(ExSupply_{HTRG})$

CHAPTER 4

RESULTS AND DISCUSSION

4.1 COMPONENT EXERGY ANALYSIS

For performing the exergy destruction analysis of complete cycle, certain state point values have been assumed such as:

Fluid temperatures

T_{20}=165 °C
T_{24}=30 °C
T_{26}=12 °C
T_{22}=30 °C
T_{21}=160 °C
T_{25}=32 °C
T_{27}=7 °C
T_{23}=35.33 °C

The atmospheric temperature and pressure are assumed to be T_o = 30 °C and P_o = 101.3 KPa. Heat exchangers efficiency is 50%.Thermodynamic state point calculations have been performed, utilizing all the equations and assumptions. These are shown in table 4.1.

Table 4.1 Thermodynamic properties at different state points

State points	Temperature (°C)	Pressure (kPa)	Mass Flow Rate (kg/s)	Vapor Quality	LiBr Mass Fraction	Enthalpy (kJ/kg)	Entropy (kJ/kgK)
1	5	0.8726	0.744	1		2510	9.024
2	38	0.8726	7.353		0.5681	97.51	0.2227
3	38	6.63	7.353		0.5681	97.51	0.2227
4	60	6.63	7.353		0.5681	141.3	0.3591
5	91.19	6.63	6.609		0.6372	235.4	0.4876
6	64.59	6.63	6.609		0.6372	186.9	0.3493
7	53.05	0.8726	0.8726	0.007196	0.6418	186.9	0.3496
8	75.96	6.63	0.2928			2642	8.511
9	38	6.63	0.744	0		159.1	0.5455
10	5	0.8726	0.744	0.0555		159.1	0.5728
11	75.96	6.63	4.863		0.5681	173.7	0.4538
12	75.96	87.69	4.863		0.5681	173.7	0.4538

13	110	87.69	4.863		0.5681	244.1	0.6454
14	157	87.69	4.412		0.6262	355.7	0.8131
15	116.5	87.69	4.412		0.6262	277.2	0.6219
16	91.19	6.63	4.412	0.01722	0.6372	277.2	0.6228
17	142.7	87.69	0.4512			2763	7.641
18	96	87.69	0.4512	0		402.2	1.261
19	38	6.63	0.4512	0.1008		402.2	1.327
20	165	700.3	74.95			697.4	1.993
21	160	700.3	74.95			675.7	1.943
22	30	101.3	107			125.8	0.4365
23	35.33	101.3	107			148.1	0.5094
24	30	101.3	100			125.8	0.4365
25	32	101.3	100			134.1	0.464
26	12	101.3	83.5			50.46	0.1804
27	7	101.3	83.5			29.51	0.1063

From the above data, the total thermal energy supplied to the absorption chiller (i.e. High temperature regenerator) is $Q_{HTRG} = m_{20}*(h_{20} - h_{21}) = 1628$ kW.

The cooling effect from the evaporator is $Q_{EVP} = m_{26}*(h_{26} - h_{27}) = 1749$ kW.

COP of the system is the ratio of the cooling effect from the evaporator to the thermal energy supplied in the high temperature regenerator.

COP=Qevap / Qgenh

COP of the system is found to be 1.074.

The total exergy supply :

$ExSupply_{HTRG} = m_{20}*[(h_{20} - h_{21}) - T_o*(S_{20} - S_{21})] = 495.8$ kW.

The total exergy loss to the environment is the sum of the exergy loss from the condenser and the exergy loss from the absorber.

$ExLoss = ExLoss_{CON} + ExLoss_{ABS}$

$ExLoss = m_{24}*[(h_{25} - h_{24}) - T_o*(S_{25} - S_{24})] + m_{22}*[(h_{23} - h_{22}) - T_o*(S_{23} - S_{22})] = 25.06$ kW

The total exergy for the recquired cooling:

$Ex_{LOAD} = m_{26}*[(h_{26}- h_{27}) -T_o*(S_{26}- S_{27})] = 126$ kW

The total exergy destruction within the absorption chiller system:

ExDes=ExSupply-Exloss-Exload= 344.74 kW

The exergy destruction in each component:

$ExDes_{EVP} = m_{26}*[(h_{26} - h_{27})-T_o*(S_{26} - S_{27})] + m_{10}*[(h_{10} - h_1)-T_o*(S_{10}-S_1)] = 30.28$ kW

$ExDes_{CON} = m_{24}*[(h_{24} - h_{25})-T_o*(S_{24} - S_{25})]+ m_8*(h_8-T_o*S_8)+ m_{19}*(h_{19} -T_o*S_{19})-m_9*(h_9 -T_o*S_9) = 19.91$ kW

$ExDes_{ABS} = m_{22}*[(h_{22} -h_{23}) -T_o*(S_{22} -S_{23})] +m_1*(h_1 -T_o*S_1) + m_7*(h_7-T_o*S_7) –m_2*(h_2 -T_o*S_2) = 125.7$ kW

$ExDes_{HTRG} = m_{20}*[(h_{20} - h_{21})-T_o*(S_{20} - S_{21})] + m_{13}*(h_{13} -T_o*S_{13}) -m_{14}*(h_{14} -T_o*S_{14}) -m_{17}*(h_{17} - T_o*S_{17}) = 47.91$ kW

$ExDes_{LTRG} = m_{17}*[(h_{17} - h_{18})-T_o*(S_{17} - S_{18})) + m_4*(h_4 -T_o*S_4)+ m_{16}*(h_{16} -T_o*S_{16}) -m_{11}*(h_{11} - T_o*S_{11})- m_5*(h_5 -T_o*S_5) -m_8*(h_8 -T_o*S_8) = 48.81$kW

$ExDes_{VALVE,L,R} = m_9*T_o*(S_{10}- S_9) = 6.16$ kW

$ExDes_{VALVE,H,R}= m_{18}*T_o*(S_{19} – S_{18}) = 8.91$ kW

$ExDes_{VALVE,L,S}= m_6*T_o*(S_7 – S_6) = 0.6007$ kW

$ExDes_{VALVE,H,S} = m_{15}*T_o*(S_{16} – S_{15}) = 1.203$ kW

$ExDes_{HTHX}=m_{12}*[(h_{12} - h_{13}) -T_o*(S_{12} - S_{13})] + m_{14}*[(h_{14} - h_{15})-T_o*(S_{14} - S_{15})] = 30.51$ kW

$ExDes_{LTHX} = m_3*[(h_3 – h_4) -T_o*(S_3 – S_4)] + m_5*[(h_5 – h_6) -T_o*(S_5 – S_6)] = 24.85$ kW

Total exergy destruction in the system:

$ExDes = ExDes_{EVP} + ExDes_{CON} + ExDes_{ABS} + ExDes_{HTRG} + ExDes_{LTRG} + ExDes_{VALVE,L,R} + ExDes_{VALVE,H,R}+ ExDes_{VALVE,L,S}+ExDes_{VALVE,H,S}+ ExDes_{LTHX} +ExDes_{HTHX} = 344.8$ kW which is equal to the exergy destruction calculated above.

The system exergetic efficiency:

$\eta_{ex} = Ex_{LOAD}/(ExSupply_{HTRG}) = 25.4\%$

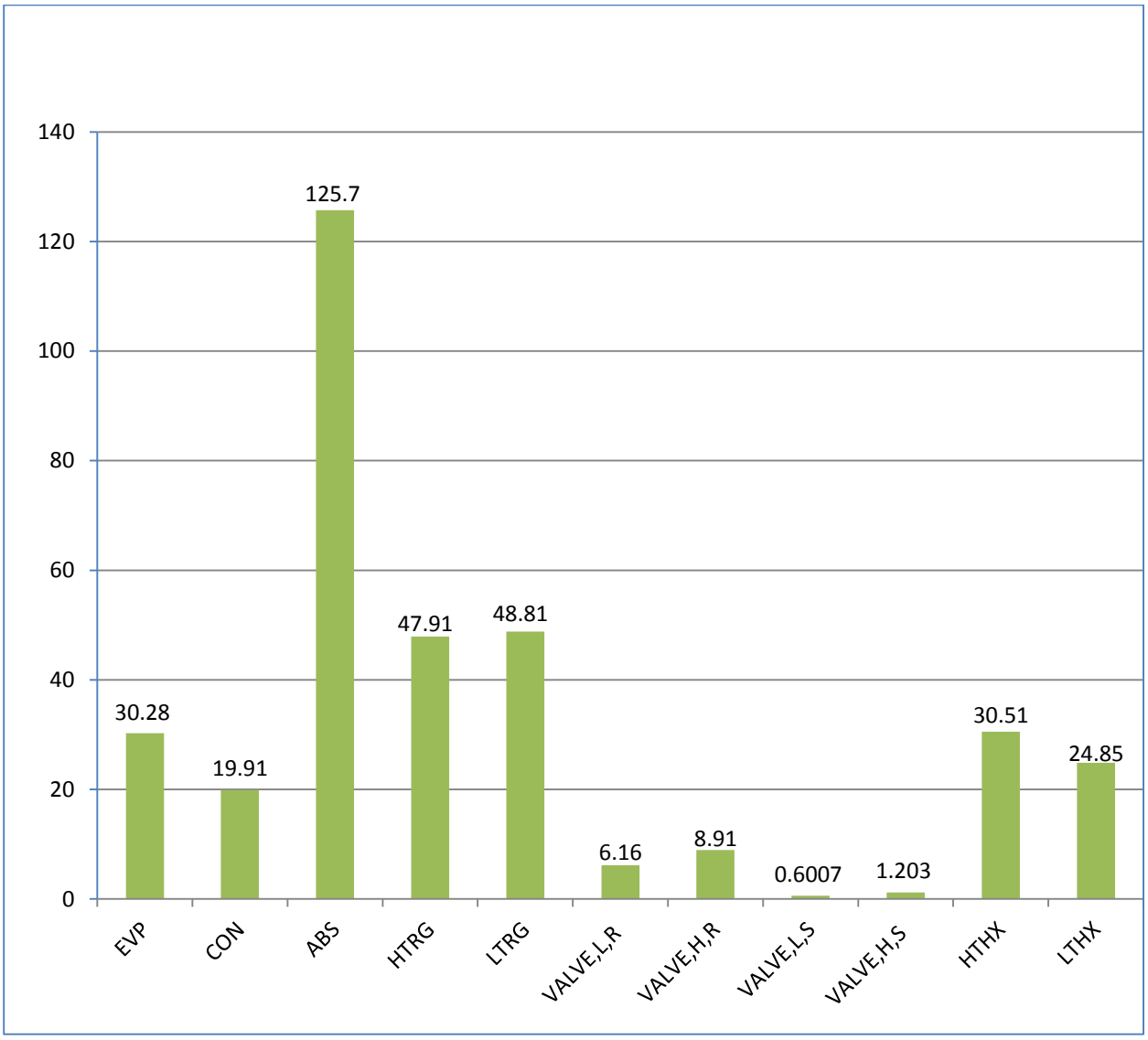

Figure 4.1 Exergy destruction (in kW) of each component in the system

It is clear that more than 70% of the total exergy supply is getting wasted in the form of exergy destruction and exergy loss to the environment. From the fig.4.1,the exergy destruction in the absorber is highest with 125.7 kW which is around 36.45% of the total exergy destruction. After the absorber, exergy destruction is higher in high temperature and low temperature regenerators with 47.91 kW and 48.81 kW respectively which is 13.89 and 14.15 % of the total exergy destruction. These three components are responsible for 70% of the total exergy destruction thus more emphasis should be given to the design of these components in order to enhance the exergy utilization.

The other components in the decreasing order of exergy destruction are high temperature heat exchanger, evaporator, low temperature heat exchanger, condenser, upper refrigerant expansion valve, lower refrigerant expansion valve, upper solution expansion valve and lower solution expansion valve with exergy destruction values 30.51, 30.28, 24.85, 19.91, 8.91, 6.16, 1.203 and 0.6007 kW respectively.

4.2 VARIATION OF COP WITH DIFFERENT TEMPERATURES

Separate graphs of the coefficient of performance are plotted against their main operating temperatures and the variation in the COP is studied.

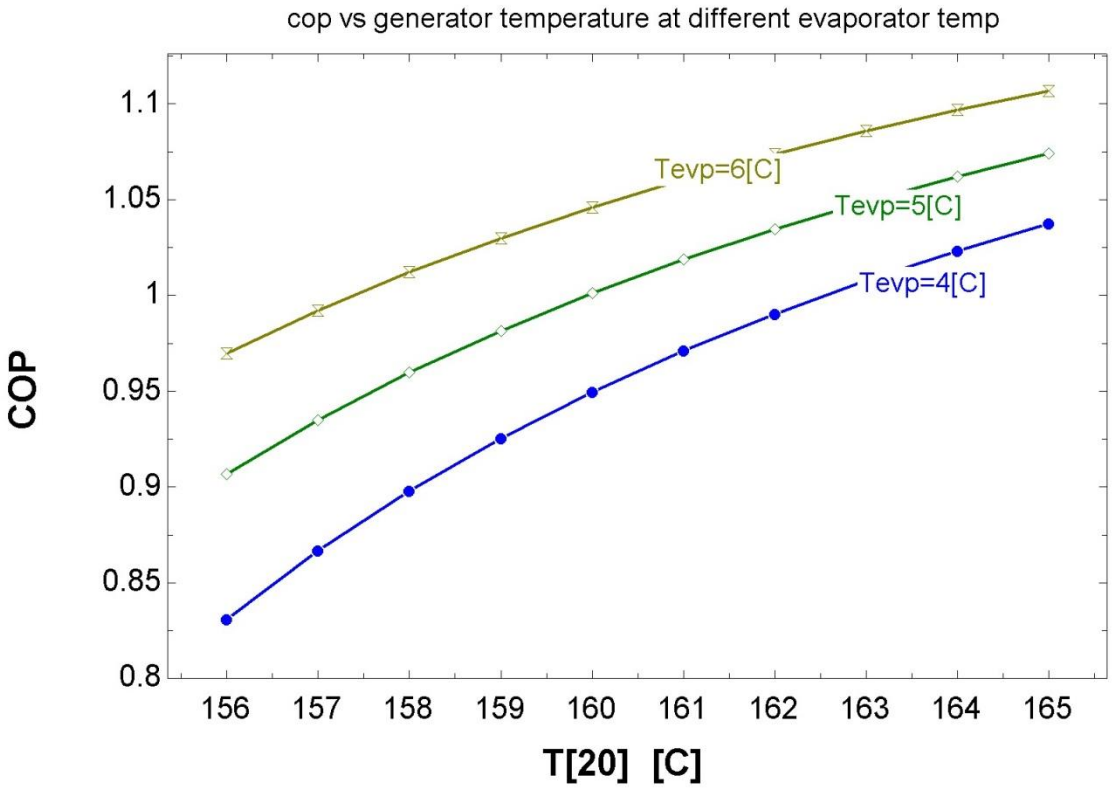

Fig 4.2 COP vs generator temperature (T_{20}) at different evaporator temperatures

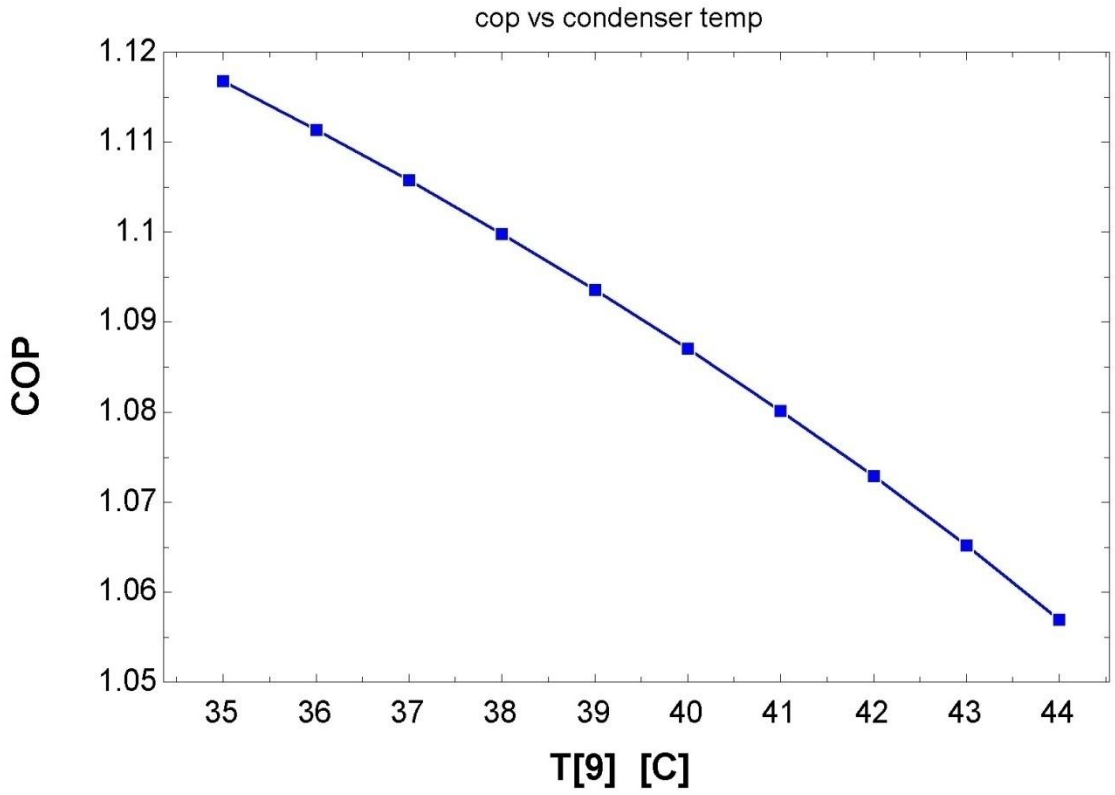

Fig 4.3 variation of COP with condenser temperature (T_9)

From the fig 4.2, it can be seen that COP of the system is increasing with generator temperature. Here the generator temperature varies from 156 to 165 °C.

At the same time, COP is also increasing with evaporator temperature which is varying from 4 to 6 °C. It should be noted that the evaporator temperature cannot be less than 1 °C.

COP of the system is decreasing with increasing condenser temperature as can be seen in fig 4.3.The condenser temperature is varying from 35 to 44 °C.

4.3 VARIATION OF EXERGY DESRUCTION WITH GENERATOR INLET TEMPERATURE.

Separate graphs of the exergy destructions are plotted against the generator inlet temperatures and the variation in the the exergy destruction of individual components and the overall system is studied. The temperature range for generator is from 156 to 165 °C.

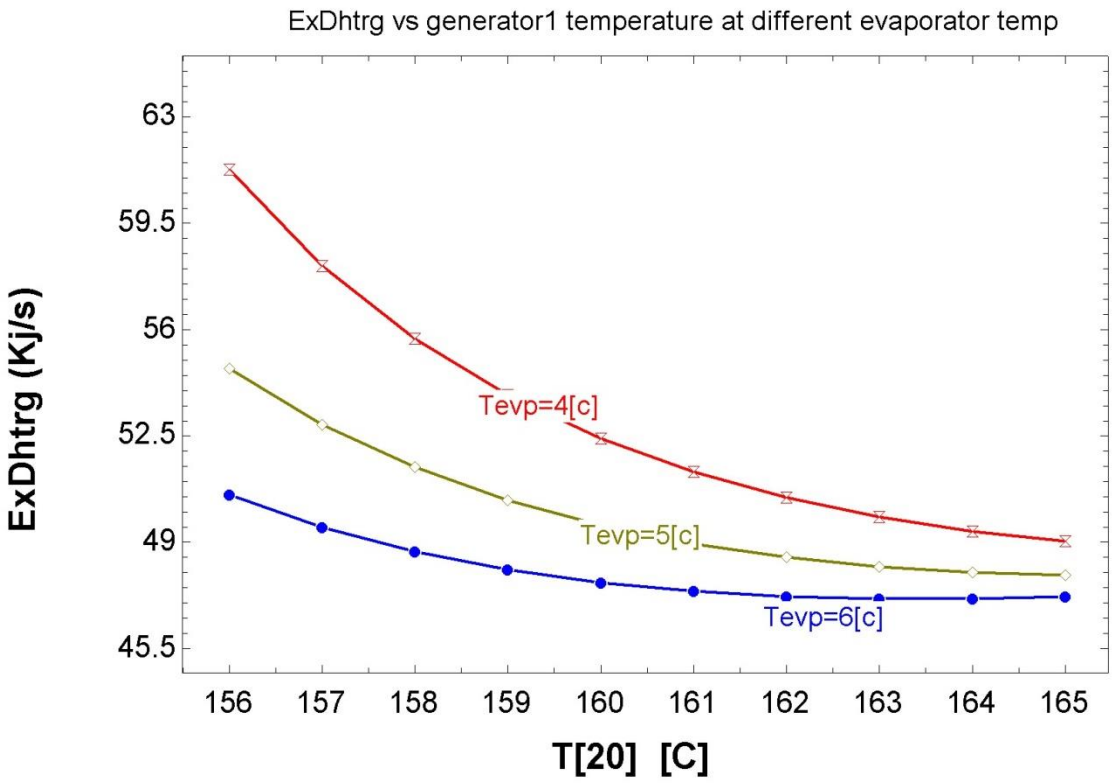

Fig 4.4 Variation of exergy destruction in High temperature regenerator with generator inlet temperature for different evaporator temperatures.

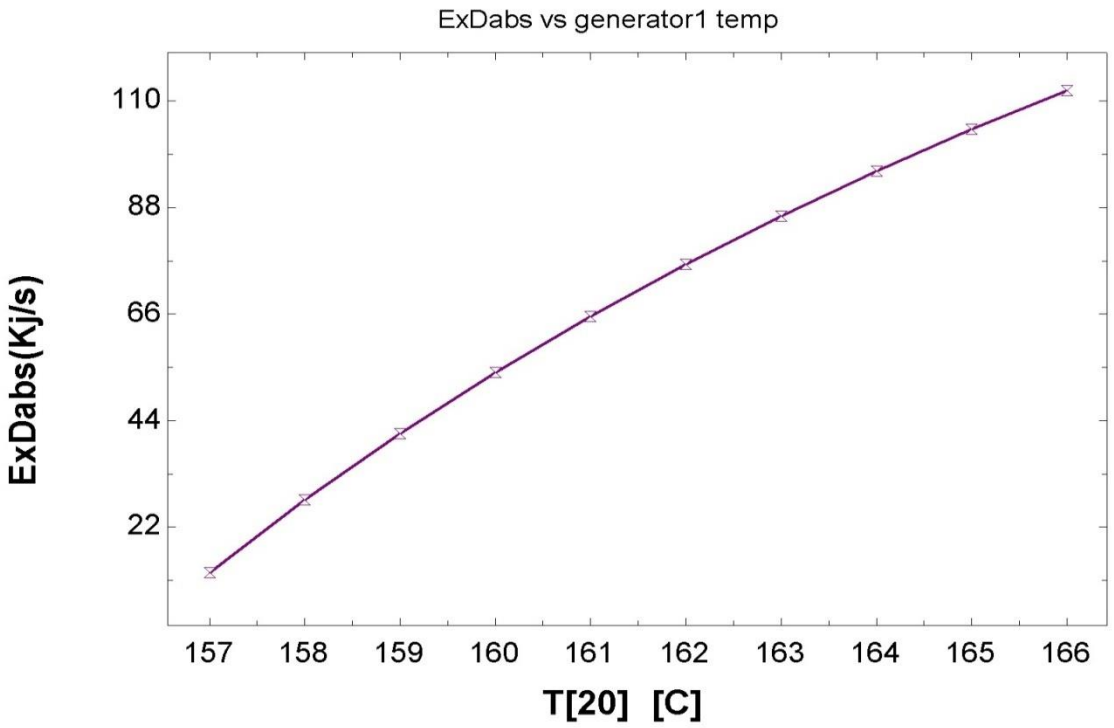

Fig 4.5 Variation of exergy destruction in absorber with generator inlet temperature.

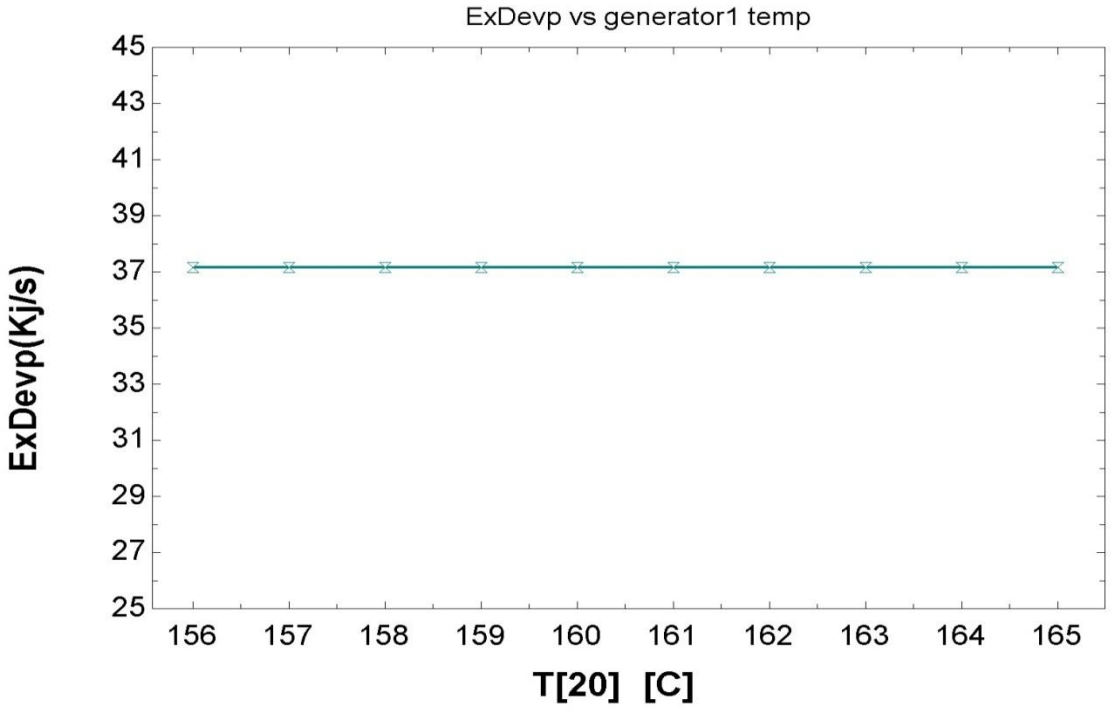

Fig 4.6 Variation of exergy destruction in evaporator with generator inlet temperature

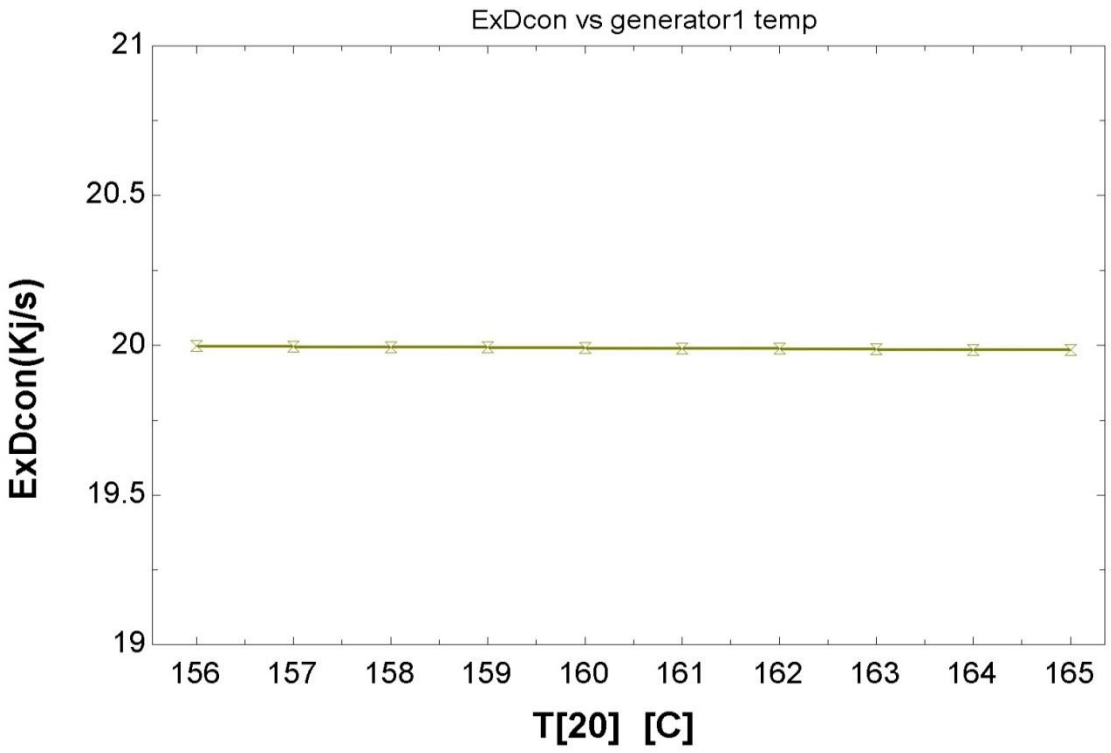

Fig 4.7 Variation of exergy destruction in condenser with generator inlet temperature

It can be seen from fig 4.4 that by increasing the generator inlet temperature while keeping the other component parameters constant, the exergy destruction is decreasing in the high temperature generator. For an increase of evaporator temperature from 4 to 6 °C, the exergy destruction is getting reduced. From the fig 4.5, it is clear that exergy destruction in the absorber is increasing with generator inlet temperature.

There is no change in the exergy destruction in the evaporator i.e. it remains constant while the generator inlet temperature is increasing(fig.4.6).Similarly the exergy destruction remains almost constant in condenser for generator inlet temperature range of 156 to 165 °C.(fig 4.7)

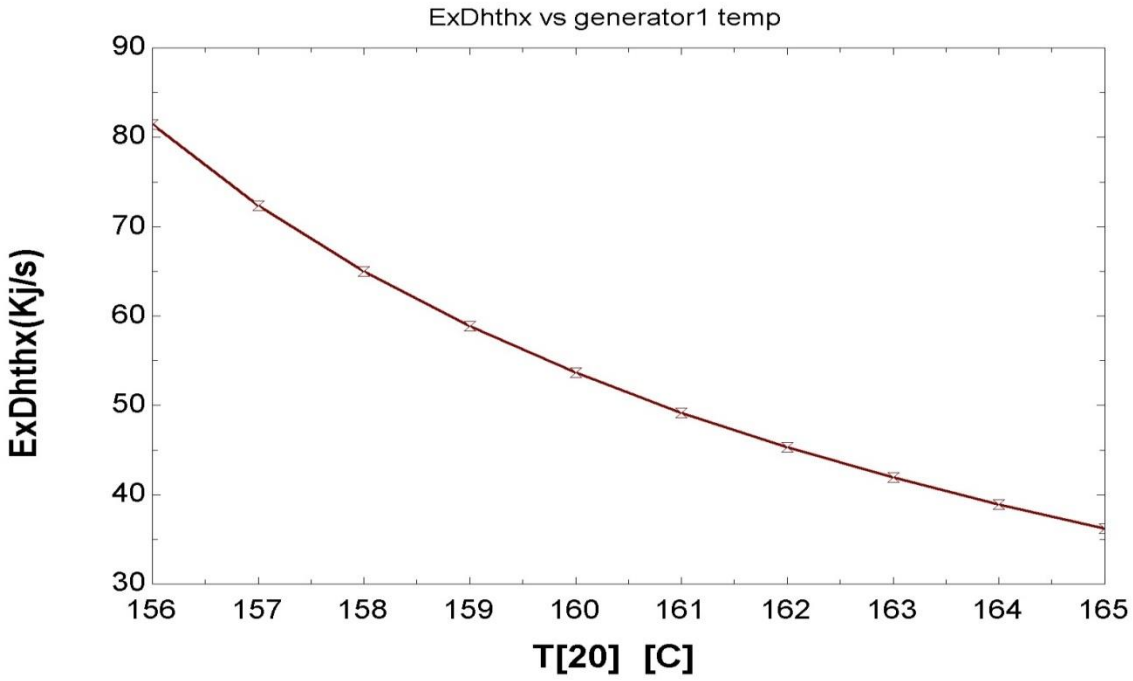

Fig 4.8 Variation of exergy destruction in high temperature heat exchanger with generator inlet temperature

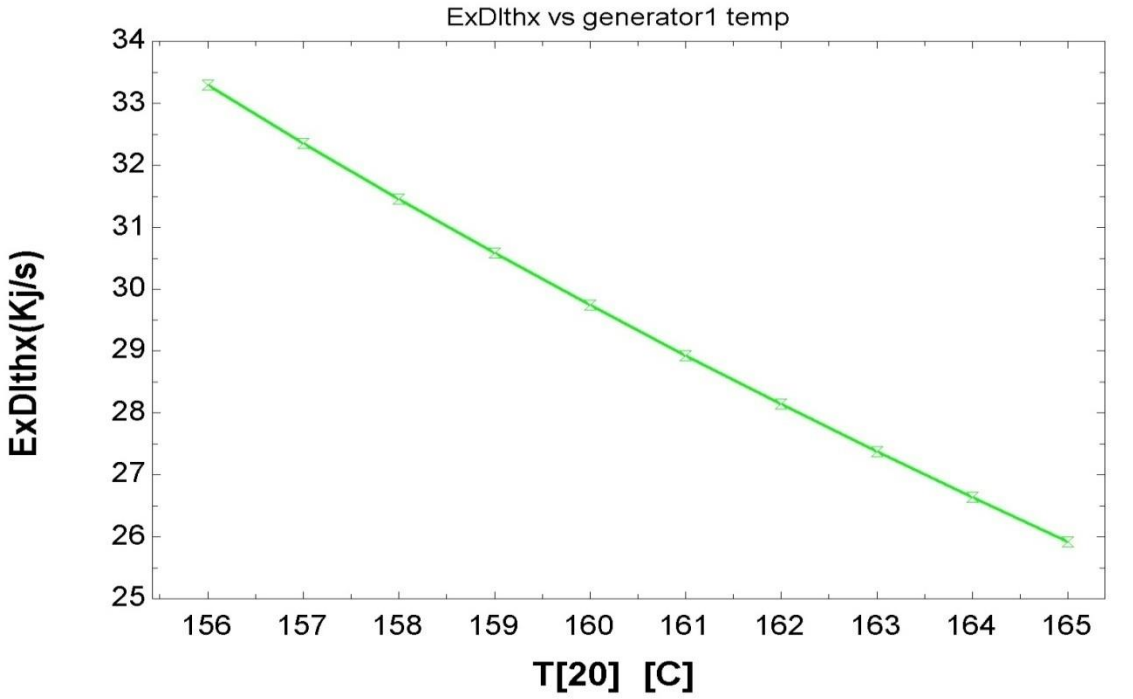

Fig 4.9 Variation of exergy destruction in low temperature heat exchanger with generator inlet temperature

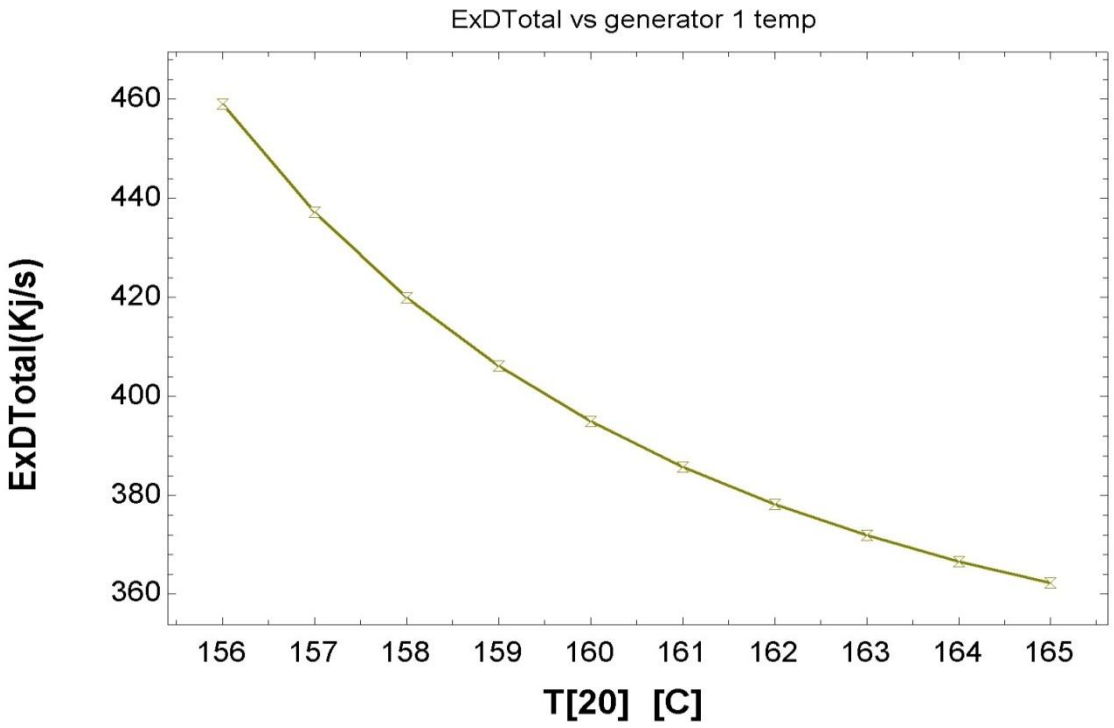

Fig 4.10 Variation of total exergy destruction in the absorption system with generator inlet temperature

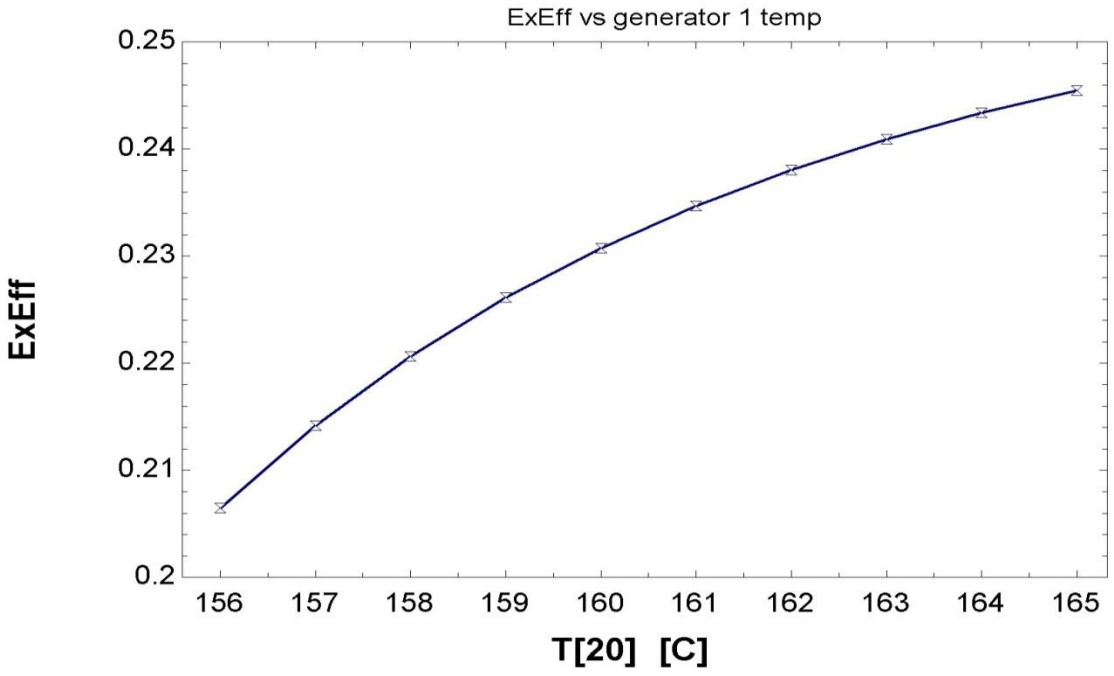

Fig 4.11 Variation of exergetic efficiency of the absorption system with generator inlet temperature

It can be seen from fig 4.8 and fig 4.9 that by increasing the generator inlet temperature, while keeping the other component parameters constant, the exergy destruction is decreasing in both the high temperature heat exchanger and low temperature heat exchanger. The decrease is higher in high temperature heat exchanger compared to the low temperature heat exchanger. From the fig 4.10, it is clear that total exergy destruction in the absorption system is decreasing from 460 to 360 kW, with increasing generator inlet temperature from 156 to 165°C.

There is a moderate increase in exergetic efficiency of the absorption system with increasing generator inlet temperature.(fig 4.11).

4.4 Variation of Exergy Destruction with Evaporator Temperature.

Separate graphs of the exergy destructions are plotted against the evaporator temperature and the variation in the the exergy destruction of individual components and the overall system is studied. The temperature range for evaporator is from 3 to 6 °C.

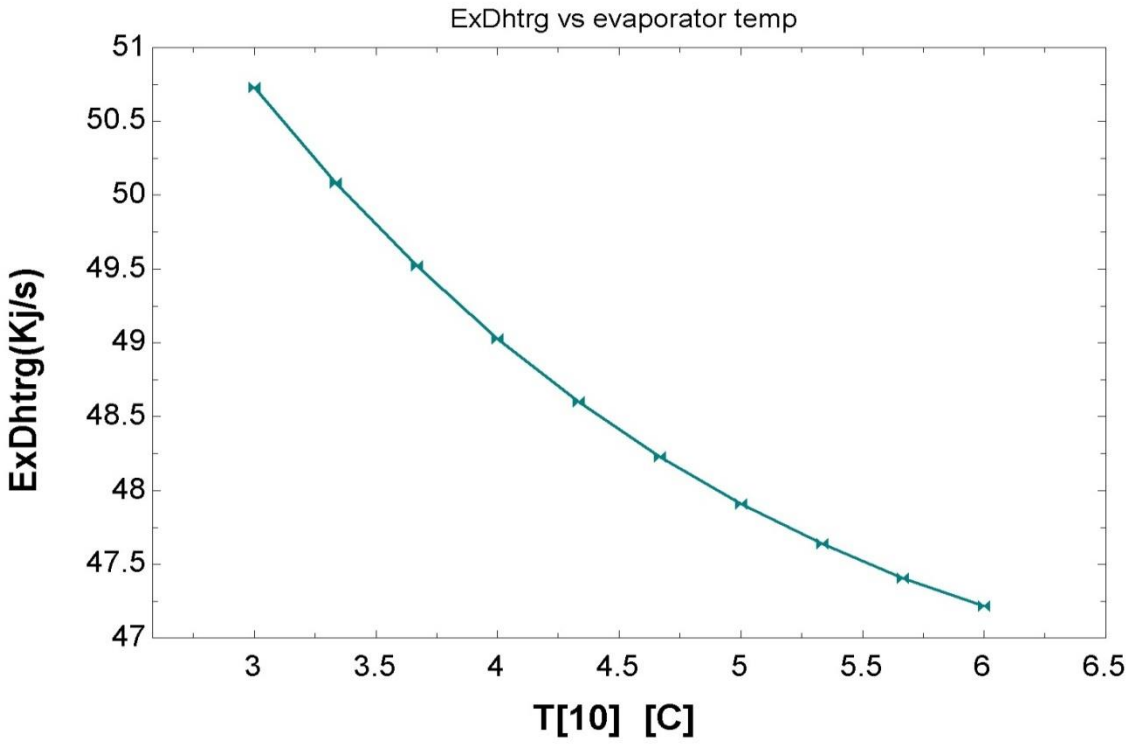

Fig 4.12 Variation of exergy destruction in High temperature regenerator with evaporator temperature.

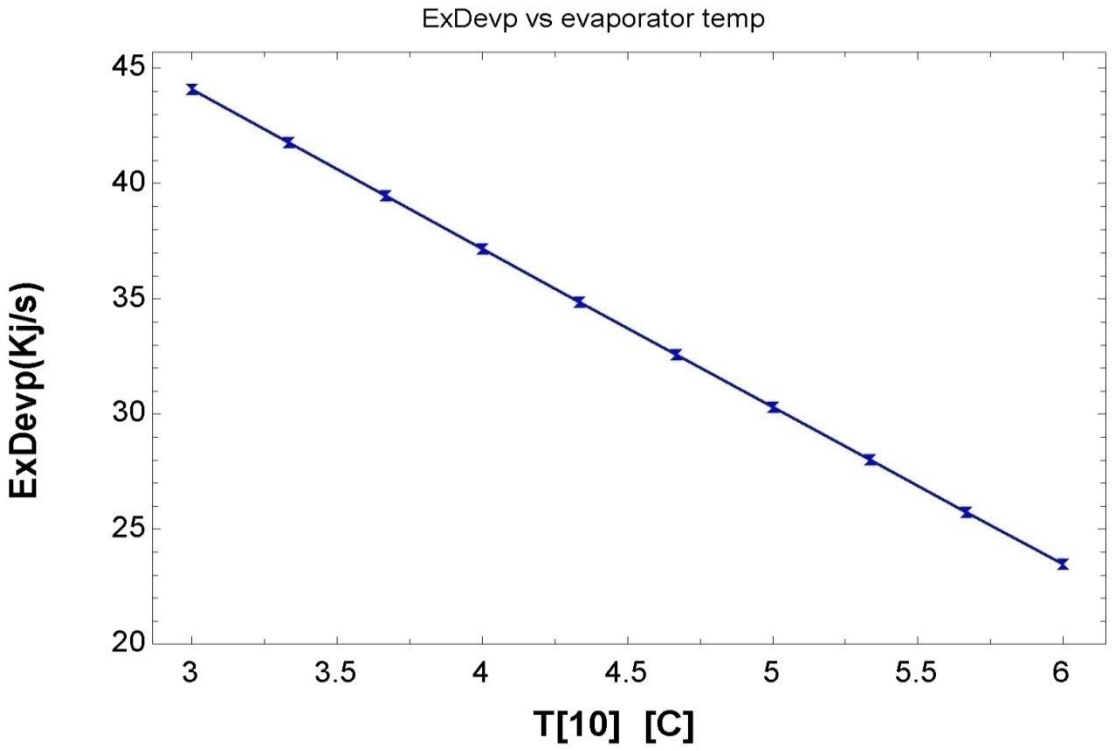

Fig 4.13 Variation of exergy destruction in evaporator with evaporator temperature.

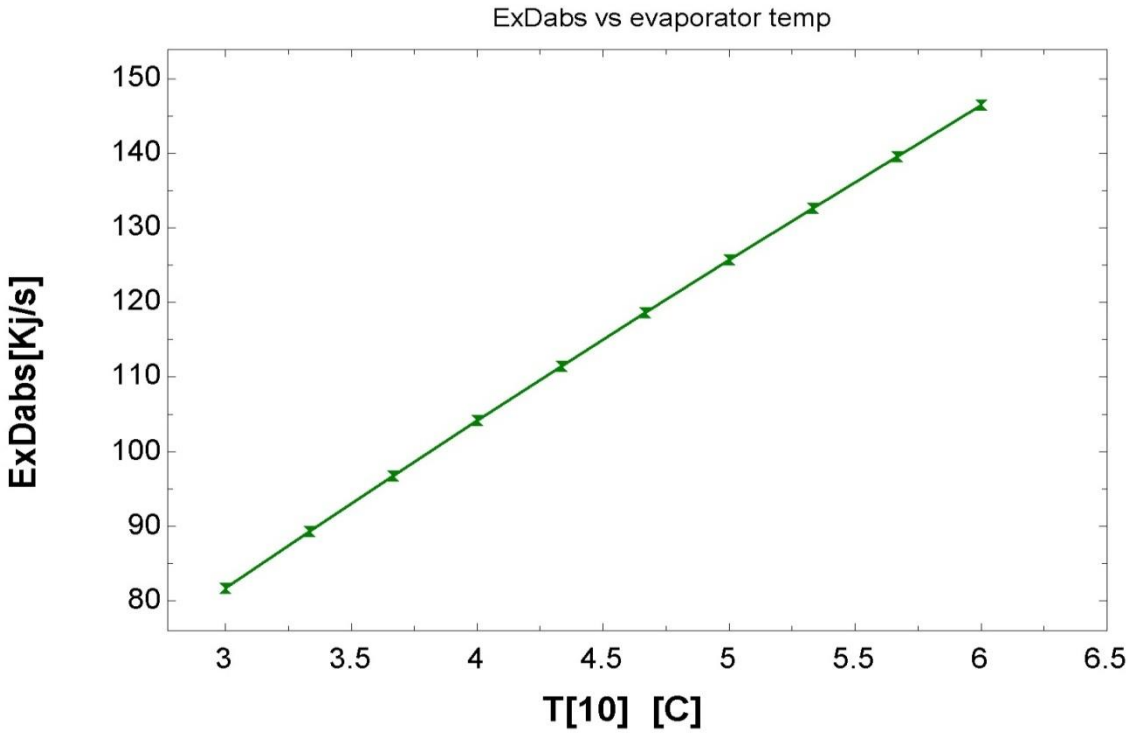

Fig 4.14 Variation of exergy destruction in absorber with evaporator temperature.

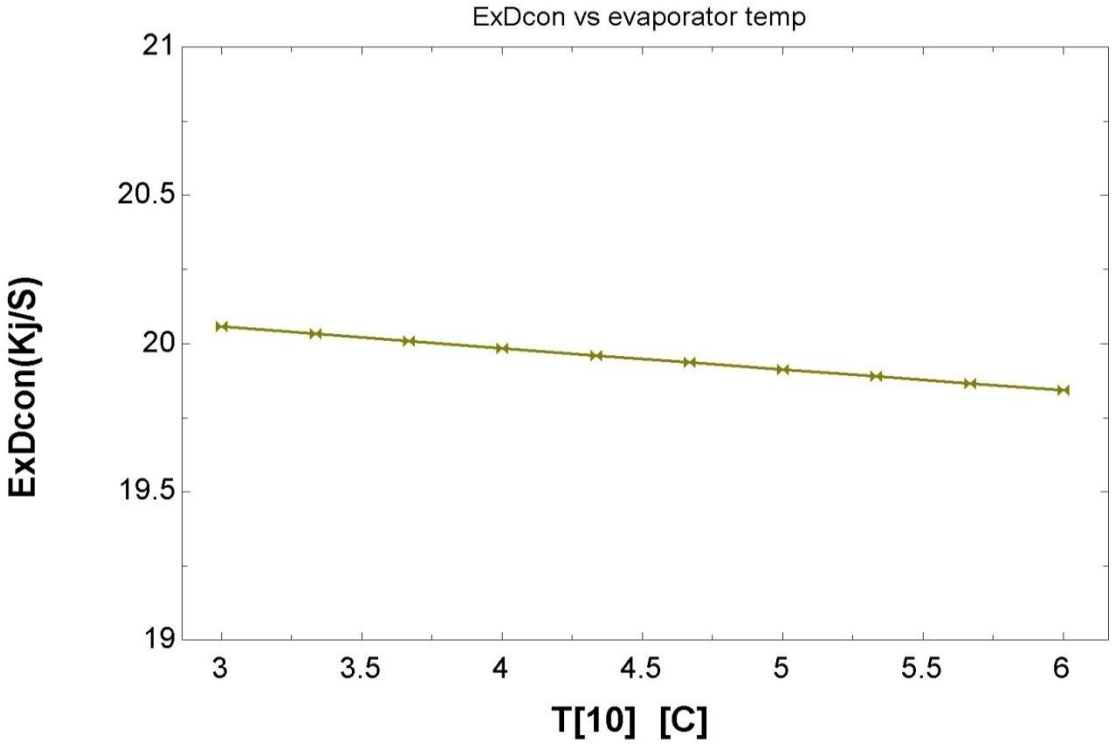

Fig 4.15 Variation of exergy destruction in condenser with evaporator temperature.

It can be seen from fig 4.12 that by increasing the evaporator temperature while keeping the other component parameters constant, the exergy destruction is decreasing slightly in the high temperature generator.

From the fig 4.13, it is clear that exergy destruction in the evaporator is decreasing with increasing evaporator temperature.

Similarly the exergy destruction in condenser is decreasing slightly for evaporator temperature range of 3 to 6 °C.(fig 4.15). There is an increase in the exergy destruction in the absorber with evaporator temperature (fig 4.14)

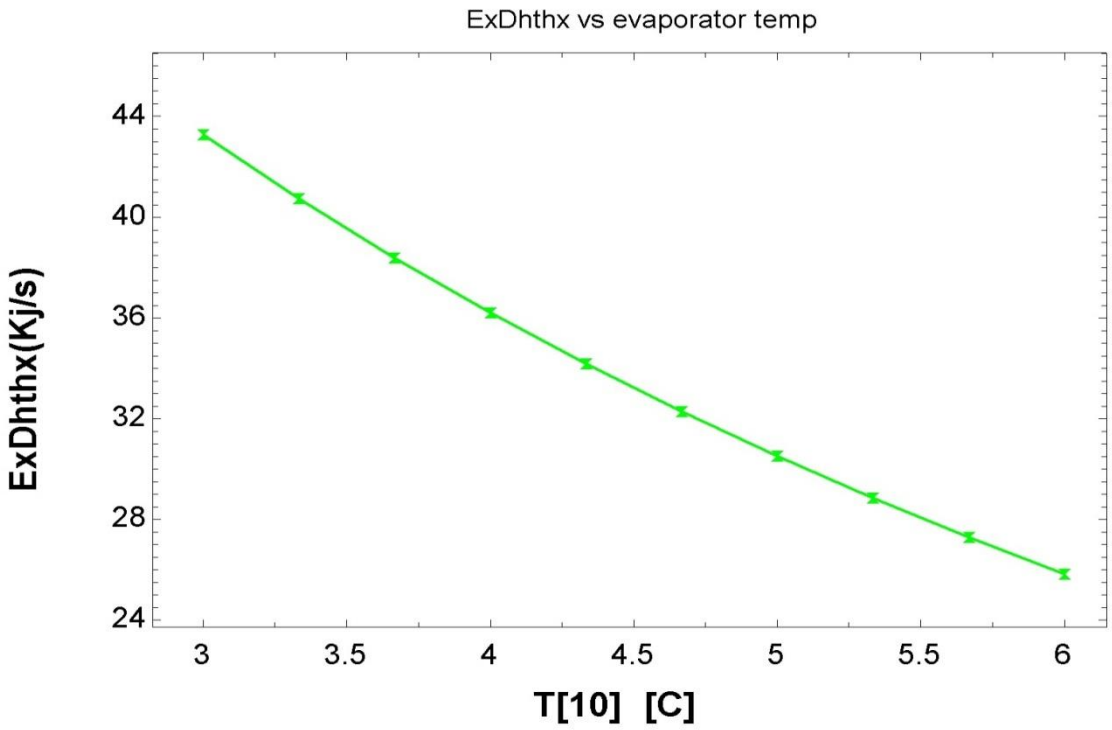

Fig 4.16 Variation of exergy destruction in high temperature heat exchanger with evaporator temperature

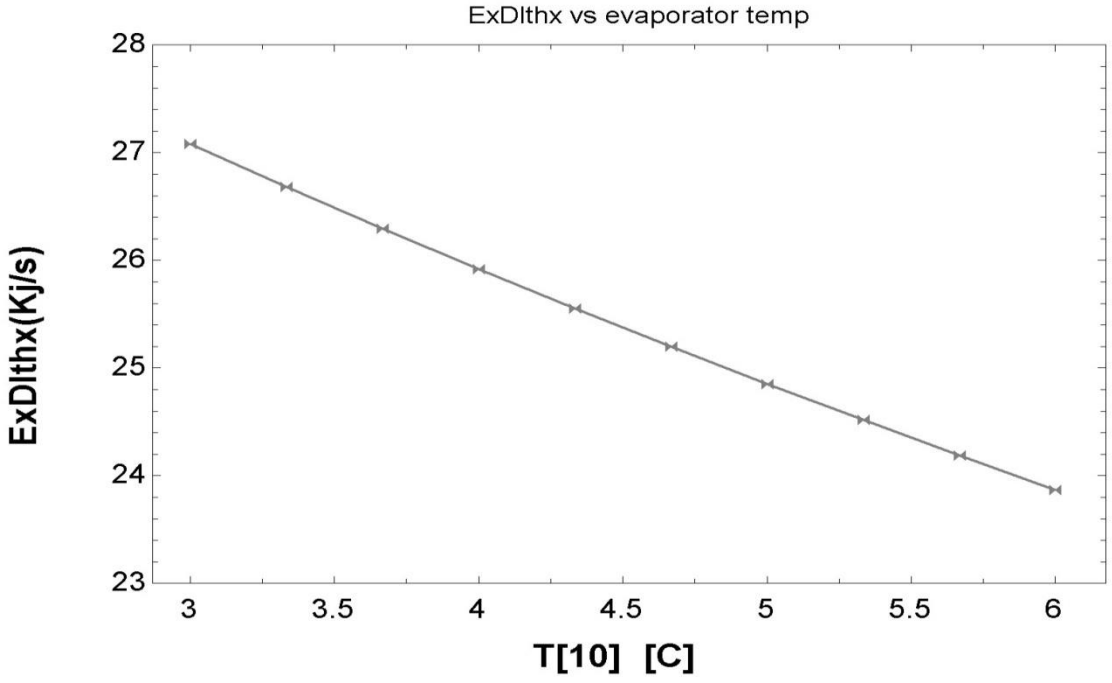

Fig 4.17 Variation of exergy destruction in low temperature heat exchanger with evaporator temperature

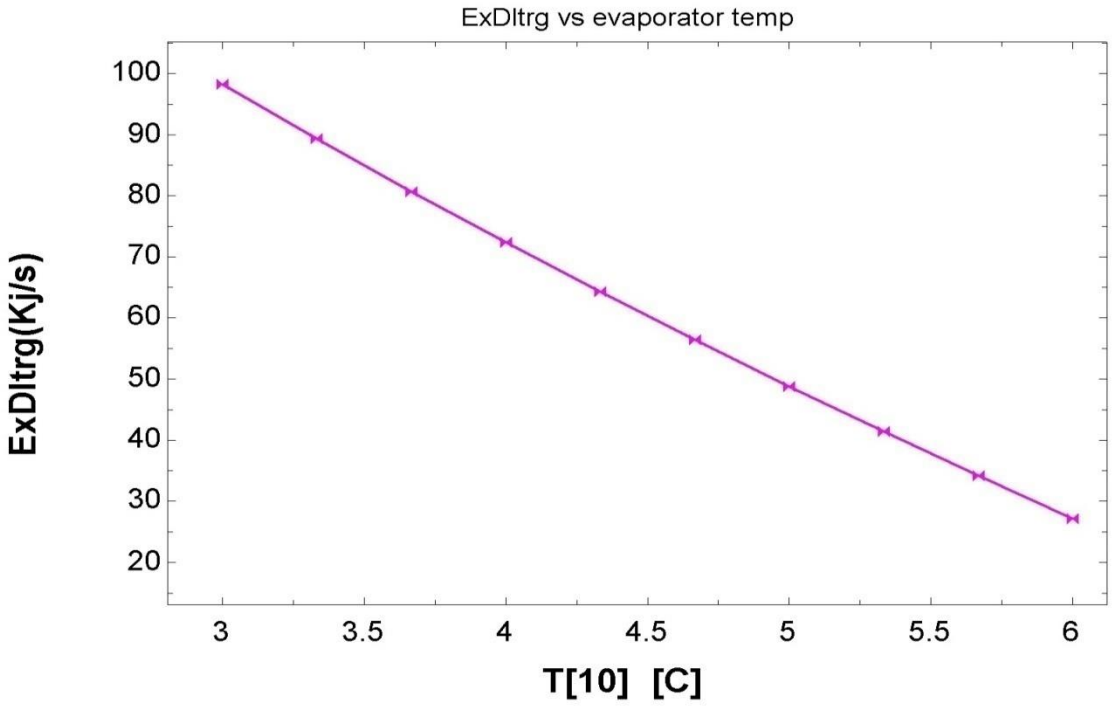

Fig 4.18 Variation of exergy destruction in low temperature regenerator with evaporator temperature

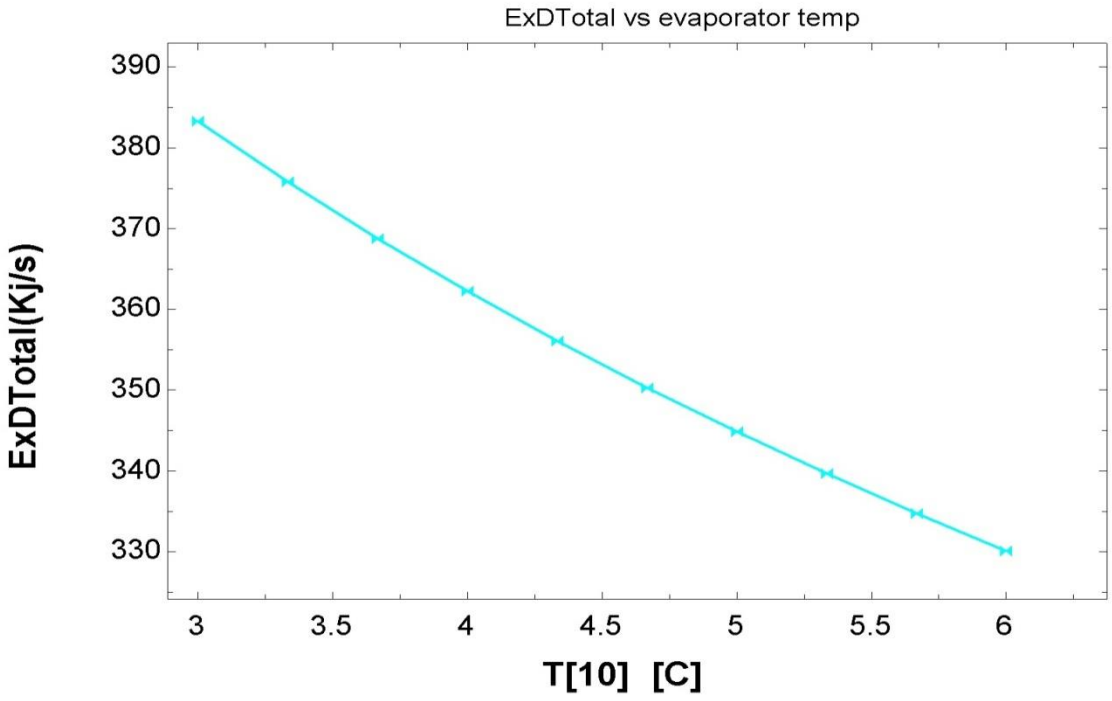

Fig 4.19 Variation of total exergy destruction in the absorption system with evaporator temperature

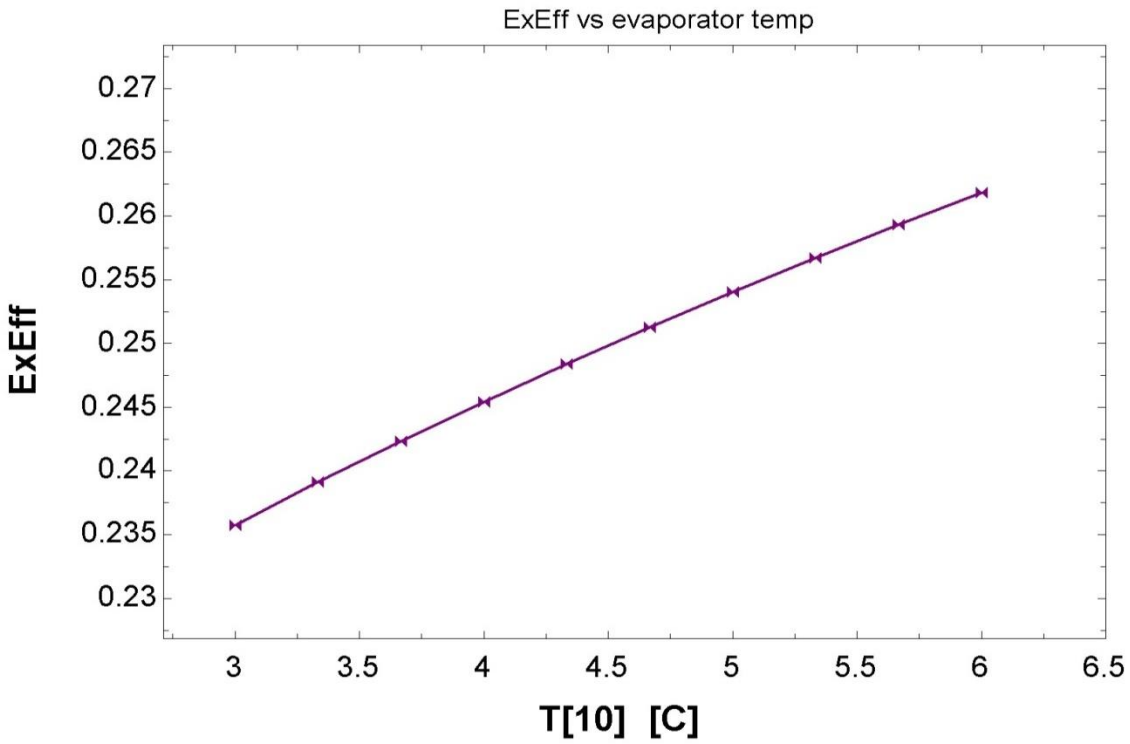

Fig 4.20 Variation of exergetic efficiency of the absorption system with evaporator temperature

It can be seen from fig 4.16 and fig 4.17 that by increasing the evaporator temperature, while keeping the other component parameters constant, the exergy destruction is decreasing in both the high temperature heat exchanger and low temperature heat exchanger. The decrease is higher in high temperature heat exchanger compared to the low temperature heat exchanger. Exergy destruction in the low temperature regenerator is dereasing sharply with evaporator temperature(fig 4.18).

From the fig 4.19, it is clear that total exergy destruction in the absorption system is decreasing from 382 to 330 kW, with increasing evaporator temperature from 3 to 6°C.There is a moderate increase in exergetic efficiency of the absorption system with increasing generator inlet temperature.(fig 4.20).

4.5 Variation of Exergy Destruction with Condenser Temperature.

Separate graphs of the exergy destructions are plotted against the condenser temperature and the variation in the the exergy destruction of individual components and the overall system is studied. The temperature range for condenser is from 35 to 44 °C.

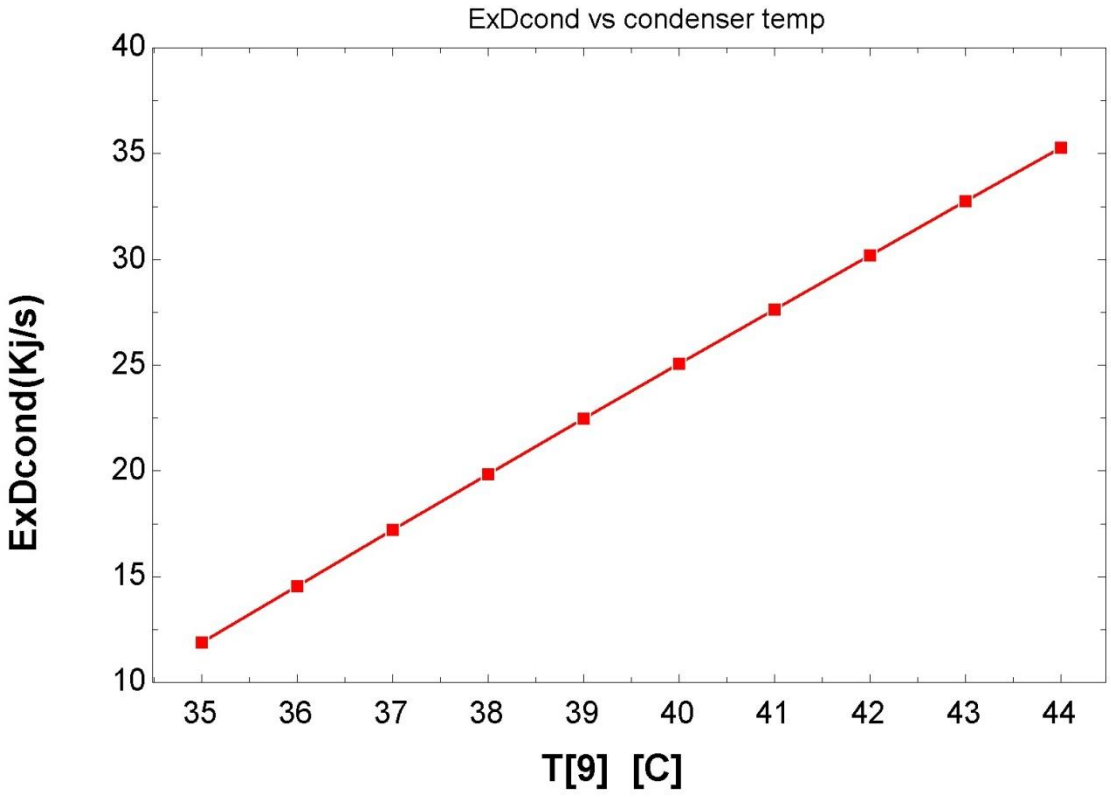

Fig 4.21 Variation of exergy destruction in condenser with condenser temperature.

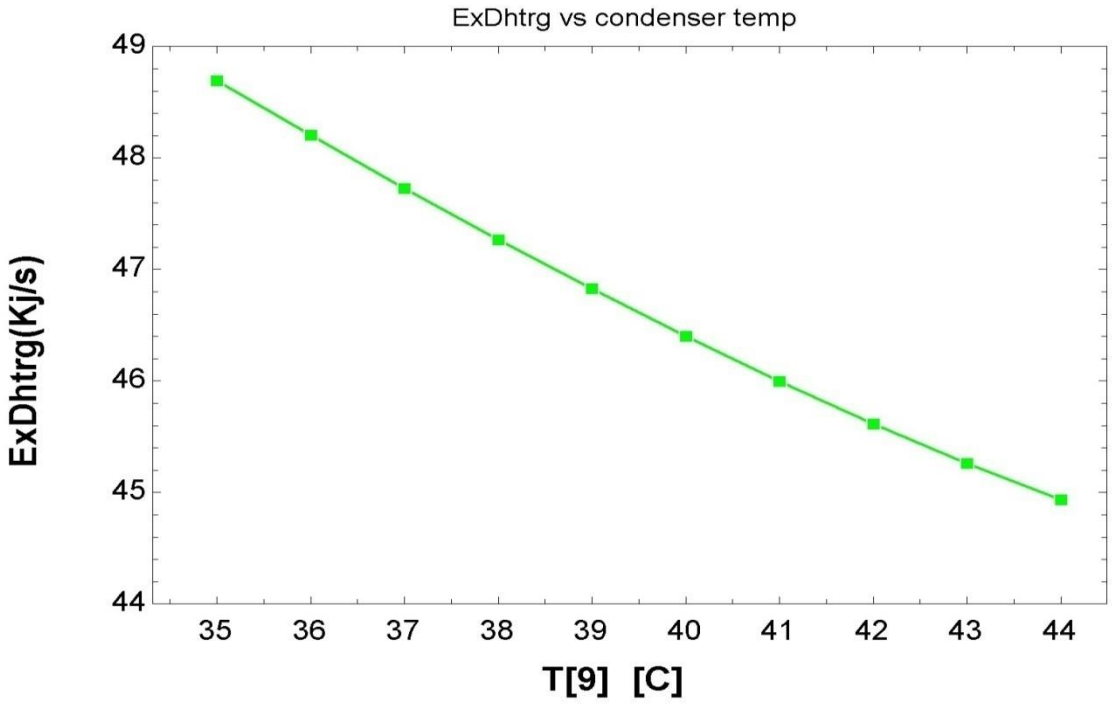

Fig 4.22 Variation of exergy destruction in High temperature regenerator with condenser temperature.

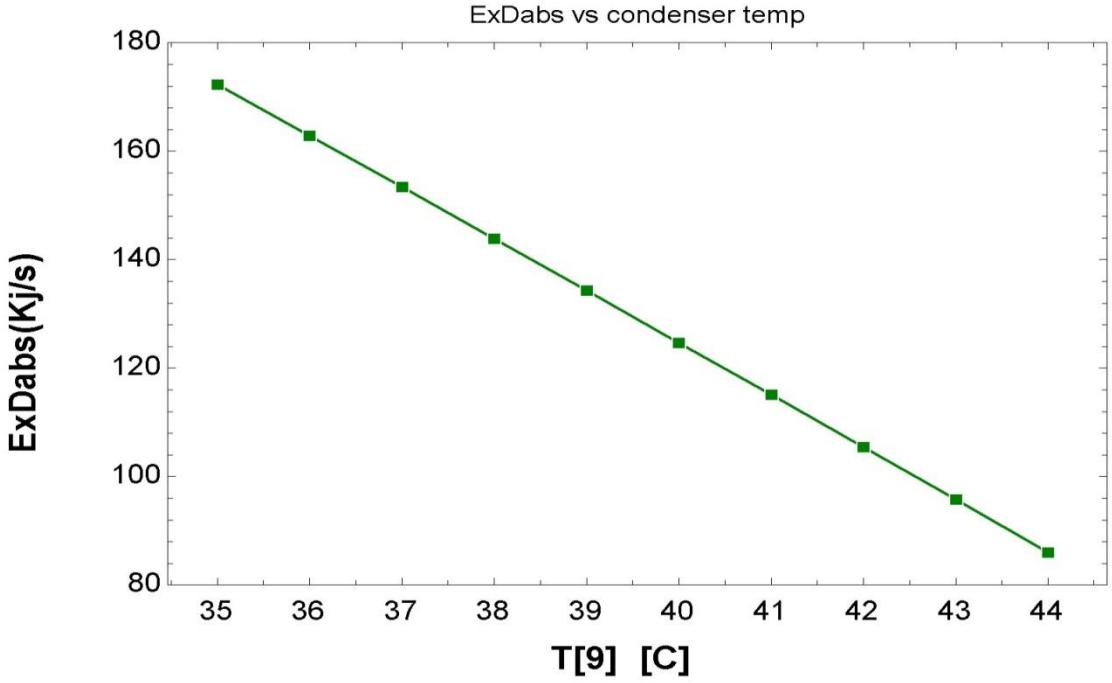

Fig 4.23 Variation of exergy destruction in absorber with condenser temperature.

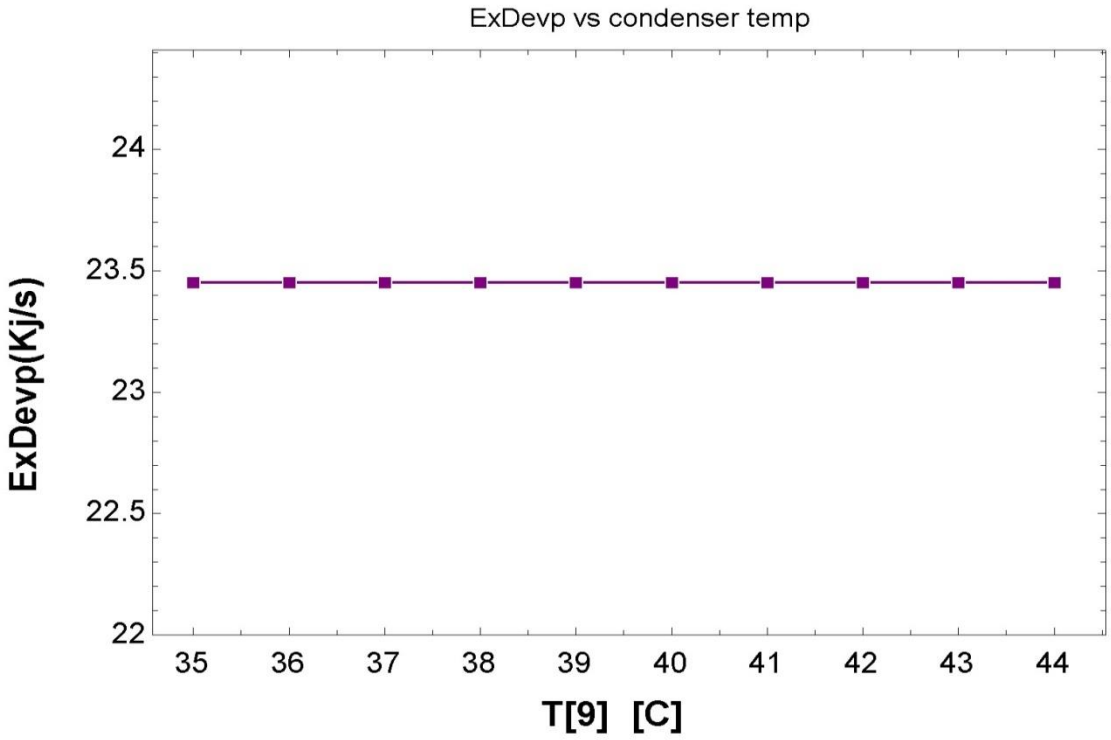

Fig 4.24 Variation of exergy destruction in evaporator with condenser temperature.

It can be seen from fig 4.22 that by increasing the condenser temperature while keeping the other component parameters constant, the exergy destruction is decreasing slightly in the high temperature generator. From the fig 4.23, it is clear that exergy destruction in the absorber is decreasing with condenser temperature.

There is no change in the exergy destruction in the evaporator i.e. it remains constant while the condenser temperature is increasing(fig.4.24).From the fig 4.21, it can be said that the exergy destruction in the condenser is increasing sharply with condenser temperature.

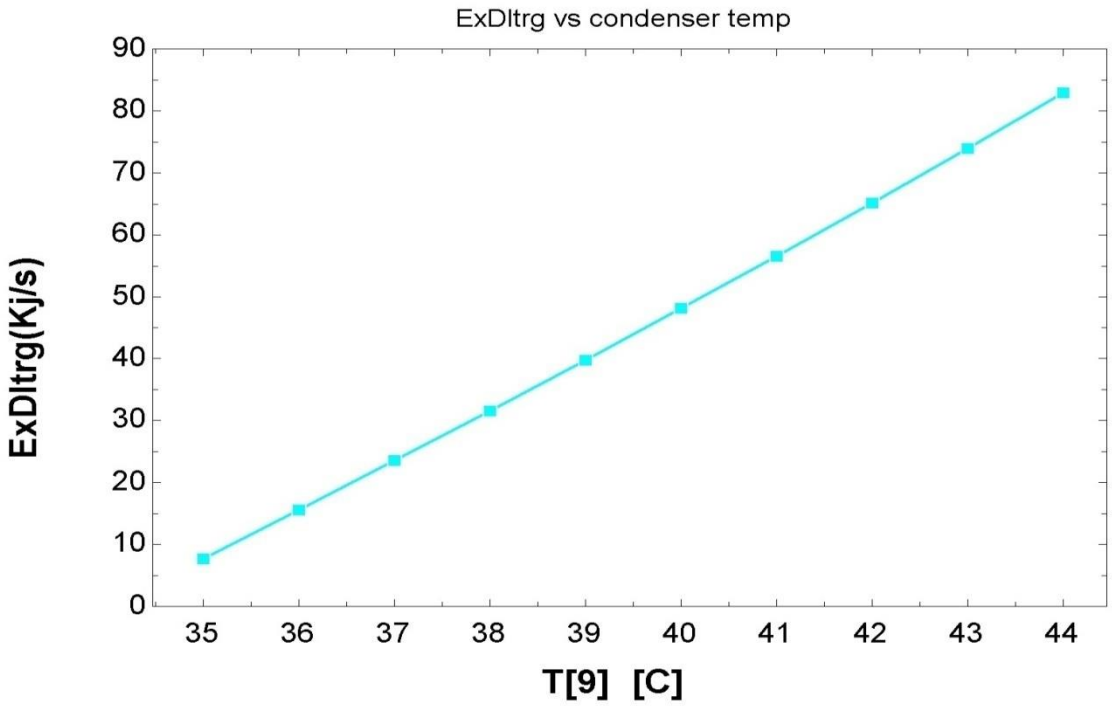

Fig 4.25 Variation of exergy destruction in low temperature regenerator with condenser temperature.

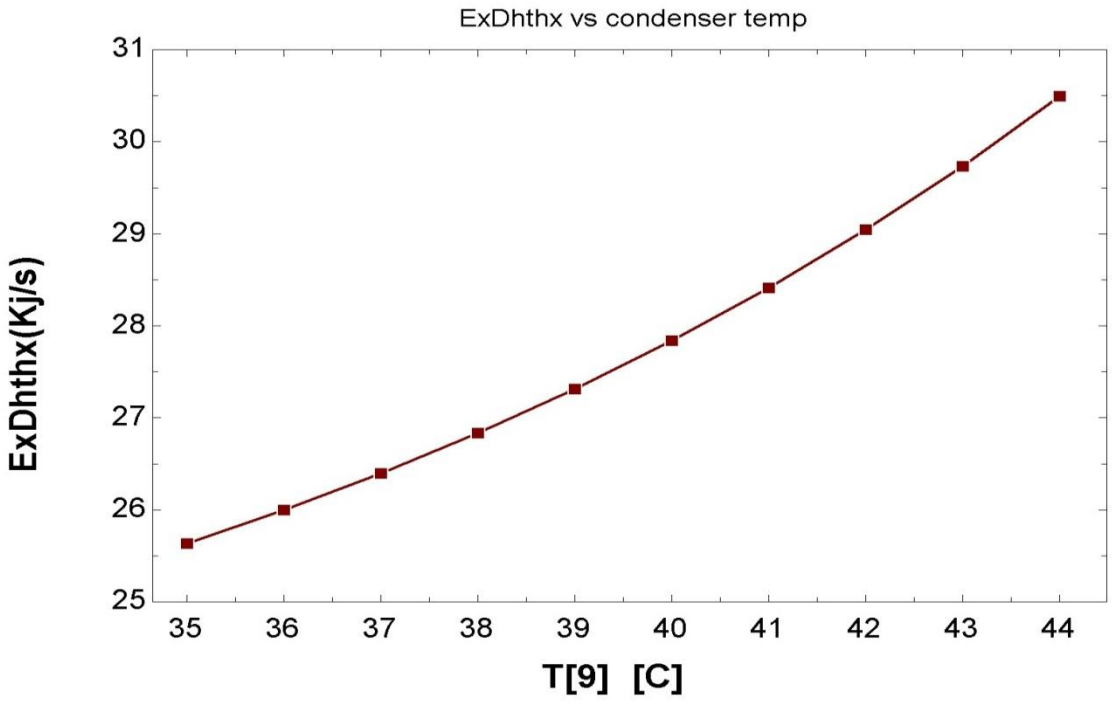

Fig 4.26 Variation of exergy destruction in high temperature heat exchanger with condenser temperature.

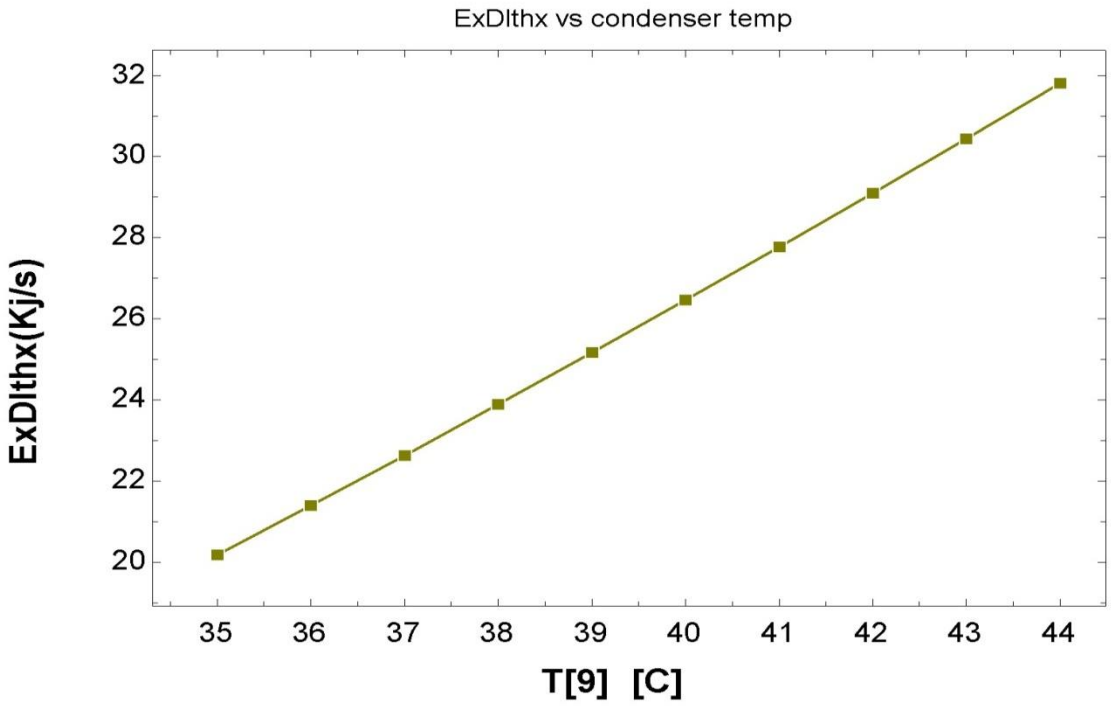

Fig 4.27 Variation of exergy destruction in low temperature heat exchanger with condenser temperature.

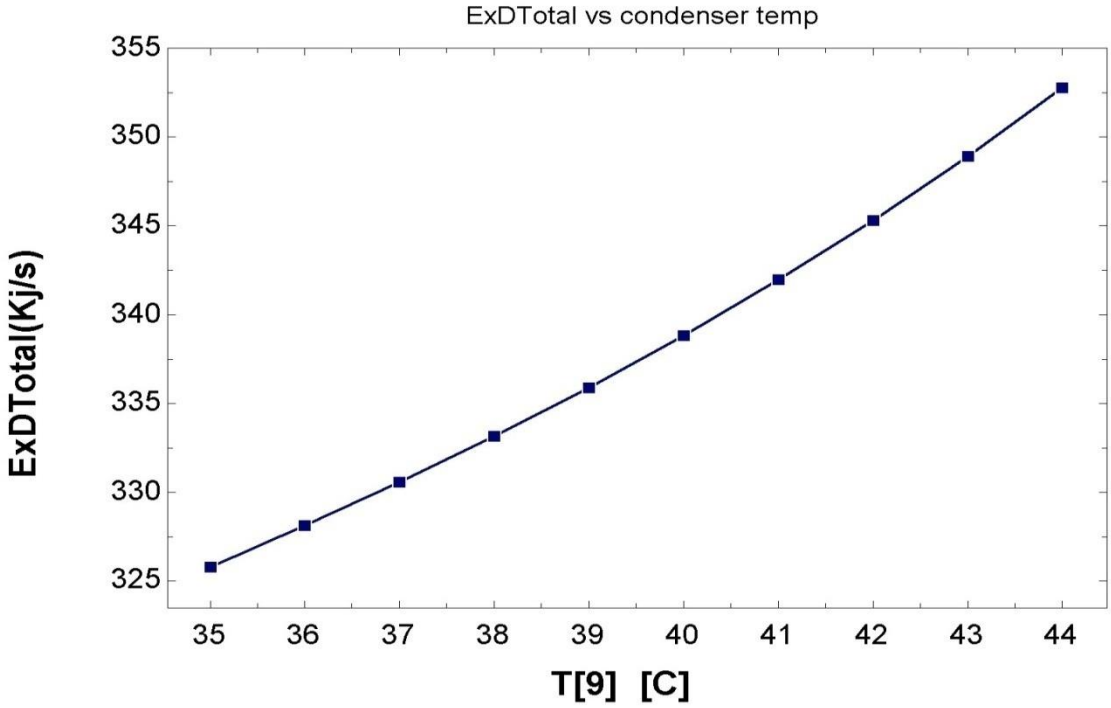

Fig 4.28 Variation of total exergy destruction in the absorption system with condenser temperature

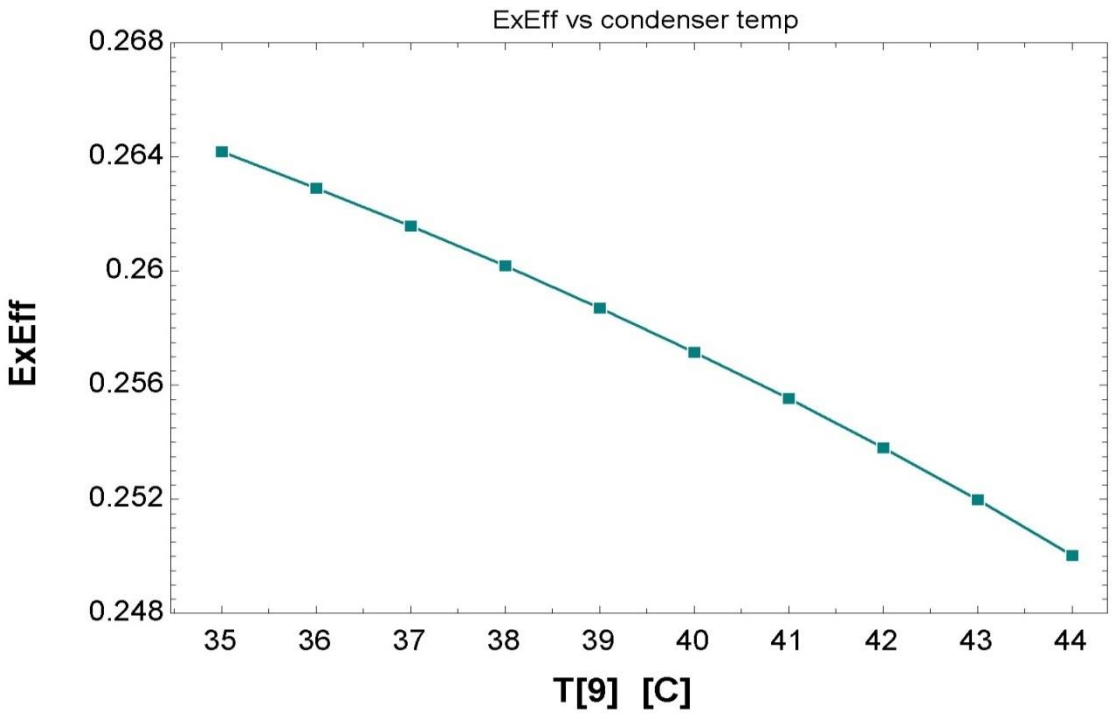

Fig 4.29 Variation of exergetic efficiency of the absorption system with evaporator temperature

It can be seen from fig 4.26 and fig 4.27 that by increasing the condenser temperature, while keeping the other component parameters constant, the exergy destruction is increasing in both the high temperature heat exchanger and low temperature heat exchanger. The increase is higher in low temperature heat exchanger compared to the high temperature heat exchanger. Exergy destruction in the low temperature regenerator is inreasing sharply with condenser temperature(fig 4.25).

From the fig 4.28, it is clear that total exergy destruction in the absorption system is increasing from 326 to 353 kW, with increasing condenser temperature from 35 to 44°C. There is a slight decrease in exergetic efficiency of the absorption system with increasing condenser temperature.(fig 4.29).

CHAPTER 5

CONCLUSION

A 500 TR double effect parallel flow absorption chiller with H_20-LiBr as refrigerant-absorbent is studied and the exergy destruction at each of its components is calculated. It is observed that more than 70% of the total exergy supply is getting wasted in the form of exergy destruction and exergy losses to the environment. The exergy destruction in the absorber is highest which is around 36.45% of the total exergy destruction. After the absorber, exergy destruction is higher in high temperature and low temperature regenerators respectively which is 13.89% and 14.15 % of the total exergy destruction. These three components, together are responsible for 70% of the total exergy destruction. Thus more emphasis should be given to the design of these three components in order to enhance the exergy utilization. The other components in the decreasing order of exergy destruction are high temperature heat exchanger, evaporator, low temperature heat exchanger, condenser, upper refrigerant expansion valve, lower refrigerant expansion valve, upper solution expansion valve and lower solution expansion valve.

The cop of the system will increase with increasing generator and evaporator temperatures respectively while it decreases with increasing condenser temperature.

The exergy destruction in the high temperature generator, high and low temperature heat exchangers and the overall system decrease with increasing generator inlet temperature while it almost remains constant in evaporator and condenser. The exergetic efficiency of the system and the exergy destruction in absorber increase with generator inlet temperature. Similarly the exergy destruction in the high temperature generator, low temperature regenerator, evaporator, condenser, high and low temperature heat exchangers and the overall system decrease with increasing evaporator temperature while the exergetic efficiency of the system and the exergy destruction in absorber increase with evaporator temperature.

The exergy destruction in the condenser, low temperature regenerator, high and low temperature heat exchangers and the overall system increase with increasing condenser temperature while the exergetic efficiency of the system and the exergy destruction in absorber and high temperature generator decrease with condenser temperature. It remains constant in evaporator.

The condenser and evaporator exergy losses are much less than generator and absorber exergy losses. The exergy losses in the solution and refrigerant expansion valves are small and negligible compared to the total exergy loss. These results can be useful in the design, control and the performance enhancement of these absorption chillers.

REFERENCES

[1] Pongsid Srikhirin, Satha Aphornratana,Supachart Chungpaibulpatana, A review of absorption refrigeration technologies, Renewable and Sustainable Energy Reviews, 5 (2001) 343–372

[2] S.C. Kaushik, A. Arora, Energy and exergy analysis of single-effect and series flow double effect water-lithium bromide absorption refrigeration systems,Int. J. Refrig. 32 (2009)

[3] Mohammad Seraj , M. Altamush Siddiqui, Performance Analysis Of Parallel Flow Single and Double Effect Absorption Cycle,IJIRSET, 2 (2013)

[4] R. Palacios Bereche1, R. Gonzales Palomino2, S. A. Nebra, Thermoeconomic Analysis of Single and Double-Effect LiBr/H2O Absorption Refrigeration System,Int.J. of Therm,12 (2009) 89-96

[5] G. Subba Rao,Vemuri Lakshminarayana, Simulation and Analysis of Biogas operated Double Effect GAX Absorption Refrigeration System,IJARME,1 (2011)

[6] C.O. Rivera, W. Rivera, Modeling of an intermittent solar absorption refrigeration system operating with ammonia-lithium nitrate mixture, Sol. Energy Mater. Sol. Cells, 76 (2003)

[7] R. Ventas, A. Lecuona, A. Zacarías, M. Venegas, Ammonia-lithium nitrate absorption chiller with an integrated low-pressure compression booster cycle for low driving temperatures, Appl. Therm. Eng. 30 (2010) 1351-1359.

[8] A. Zacarías, M. Venegas, R. Ventas, A. Lecuona, Experimental assessment of ammonia adiabatic absorption into ammonia-lithium nitrate solution using a flat fan nozzle, Appl. Therm. Eng. 31 (2011) 3569-3579.

[9] W. Rivera, G. Moreno-Quintanar, C.O. Rivera, R. Best, F. Martínez, Evaluation of a solar intermittent refrigeration system for ice production operating with ammonia/lithium nitrate Sol. Energy, 85 (2011) 38-45.

[10] A. Acuña, N. Velázquez, J. Cerezo, Energy analysis of a diffusion absorption cooling system using lithium nitrate, sodium thiocyanate and water as absorbent substances and ammonia as the refrigerant, Appl. Therm. Eng., 51(2013) 1273-1281.

[11] C. Vasilescu, C.I. Ferreira, Solar driven double-effect absorption cycles for subzero temperatures, Int. J. Refrig. (2013), http://dx.doi.org/10.1016/j.ijrefrig.2013.09.034.

[12] Z. Wan, S. Shu, X. Hu, Novel high-efficient solar absorption refrigeration cycles, J. Huazhong Univ. Sci. Technol. 34 (2006) 85-87.

[13]Muhsin Kilic,Omer Kaynakli, Second law-based thermodynamic analysis of Water-lithium bromide absorption refrigeration system, Energy 32 (2007)1505-1512.

[14] B.H. Gebreslassie, M. Medrano, D. Boer, Exergy analysis of multi-effect water- LiBr absorption systems: from half to triple effect, Renewable Energy 35 (2010) 1773-1782.

[15] Cătălina VASILESCU, Dragoş HERA, Carlos INFANTE FERREIRA, Model for double effect absorption refrigeration cycle, D U T, DELFT, The Netherlands(2011)

[16]C.O. Rivera, W. Rivera, Modeling of an intermittent solar absorption refrigeration system operating with ammonia-lithium nitrate mixture, Sol. Energy Mater. Sol. Cells, 76 (2003)

[17]www.sciencedirect.com

[18] www.elsevier.com